Shannon and entanglement entropies of one- and two-dimensional critical wave functions

Jean-Marie Stéphan,[1] Shunsuke Furukawa,[2] Grégoire Misguich,[1] and Vincent Pasquier[1]

[1]*Institut de Physique Théorique, CEA, IPhT, CNRS, URA 2306, F-91191 Gif-sur-Yvette, France*
[2]*Condensed Matter Theory Laboratory, RIKEN, Wako, Saitama 351-0198, Japan*

We study the Shannon entropy of the probability distribution resulting from the ground-state wave function of a one-dimensional quantum model. This entropy is related to the entanglement entropy of a Rokhsar-Kivelson-type wave function built from the corresponding two-dimensional classical model. In both critical and massive cases, we observe that it is composed of an extensive part proportional to the length of the system and a subleading universal constant S_0. In $c=1$ critical systems (Tomonaga-Luttinger liquids), we find that S_0 is a simple function of the boson compactification radius. This finding is based on a field-theoretical analysis of the Dyson-Gaudin gas related to dimer and Calogero-Sutherland models. We also performed numerical demonstrations in the dimer models and the spin-1/2 *XXZ* chain. In a massive (crystal) phase, S_0 is related to the ground-state degeneracy. We also examine this entropy in the Ising chain in a transverse field as an example showing a $c=1/2$ critical point.

I. INTRODUCTION

There has been growing interest in quantifying entanglement in extended quantum systems to detect nontrivial correlations existing in many-body ground states.[1] A useful measure of entanglement is the von Neumann entanglement entropy $S^{\mathrm{vN}}(A) := -\mathrm{Tr}\,\rho_A \log \rho_A$, defined from the reduced density matrix ρ_A of a subsystem A. (We use the natural logarithm). Its novelty lies in its universal behavior reflecting the long-distance nature of the system. In one-dimensional (1D) critical systems, for instance, the entanglement entropy of a long interval of length ℓ shows a universal scaling[2–5] $S^{\mathrm{vN}}(A) \simeq \frac{c}{3}\log \ell + \mathrm{const}$, where c is the central charge of the conformal field theory (CFT) describing the long-distance correlations. Possible further information of CFT can be encoded in a multi-interval entanglement entropy.[6–8] As another example, the existence of topological order in gapped systems can be detected by measuring a constant contribution to the entanglement entropy[9,10] (with recent applications to fractional quantum Hall states[11,12] and $\mathbb{Z}_2$ spin liquids[13–17]).

Here we introduce an *apparently* different entropy as follows. Consider a 1D quantum model and its ground state $|g\rangle$. If one chooses an orthogonal basis $\{|i\rangle\}$ of the Hilbert space, one gets a set of probabilities $p_i := |\langle i|g\rangle|^2$, from which a Shannon entropy can be defined,

$$S := -\sum_i p_i \log p_i. \tag{1}$$

Note that this entropy depends on the choice of basis. For a U(1)-symmetric model with the conservation of the particle number or the magnetization, we use the local particle occupations $\{n_j\}$ or magnetizations $\{\sigma_j^z\}$ to define the basis. The entropy S is small when the wave function $|g\rangle$ is dominated by a particular crystal state $|i_0\rangle$. It becomes larger as more basis states contribute to the wave function due to quantum fluctuations. Thus, this entropy quantifies quantum fluctuations or entanglement occurring in the given basis. Like other entanglement measures, we will see that the scaling of

this entropy is controlled by the essential long-distance nature of the system. We note that a similar entropy also appears in the context of dynamical systems,[18,19] where it is used to quantify chaos.[20]

At the same time, this entropy has an interpretation as the entanglement entropy of a two-dimensional (2D) quantum state, as we describe in detail in Sec. II. The basic idea goes as follows. A 1D quantum Hamiltonian on a ring is related to a 2D classical model on a cylinder in the transfer matrix formalism. Then a Rokhsar-Kivelson (RK)-type wave function[21,22] $|\mathrm{RK}\rangle$ can be constructed from this 2D classical model. One can show that in the limit of a long cylinder, the entropy S defined in Eq. (1) is precisely the entanglement entropy $S^{\mathrm{vN}}(A)$ of the 2D RK state $|\mathrm{RK}\rangle$ for a half-cylinder A shown in Fig. 1. More specifically, each probability p_i becomes an eigenvalue of the reduced density matrix ρ_A. This correspondence allows us to apply a simpler 1D picture to study the universal behavior of entanglement entropy in 2D critical systems, a very active subject in recent literature.[23–25]

The purpose of the present paper is to unveil the generic scaling properties of the Shannon entropy [Eq. (1)] of 1D
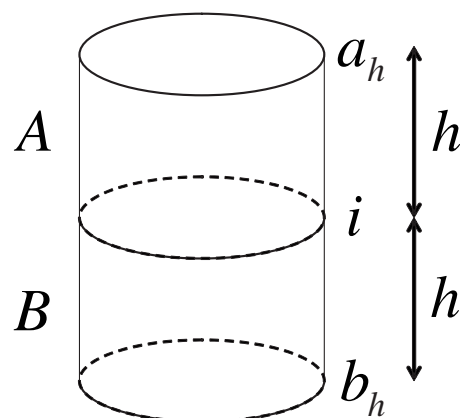
FIG. 1. Two dimensional system with a cylinder geometry, divided into upper and lower parts, A and B.

ground states $|g\rangle$ as a function of the ring length L. This amounts to studying the entanglement entropy S^{vN} of 2D RK states $|RK\rangle$ defined on a cylinder of circumference L. In both critical and massive systems, we observe that for large L, the entropy is composed of an extensive part proportional to L and a subleading constant

$$S(L) = \alpha L + S_0 + o(1). \tag{2}$$

The extensive part αL simply reflects the fact that a generic wave function $|g\rangle$ spreads over an exponentially large number of microscopic configurations. In terms of the 2D entanglement entropy, this can be interpreted as a boundary contribution. Here, we are however interested in the subleading constant S_0. As we will see, S_0 is universal and is determined by the basic properties of critical or massive systems.

Our primary interest lies in the situation where a 1D quantum or 2D classical system (used to build a RK state) is described by a $c=1$ massless bosonic field theory [Tomonaga-Luttinger liquid (TLL)] with the Euclidean action

$$\mathcal{A}[\phi] = \frac{1}{8\pi} \int \int dx dy [(\partial_x \phi)^2 + (\partial_y \phi)^2]. \tag{3}$$

Here the bosonic field is compactified on a circle: $\phi \equiv \phi + 2\pi R$. The boson compactification radius R is an important scale-invariant number which controls the power-law behavior of various physical quantities.[26] We find that S_0 is given by a simple function of the radius

$$S_0 = \log R - \frac{1}{2}. \tag{4}$$

We present detailed analyses to establish this result. In Sec. III, we study the Dyson-Gaudin Coulomb gas model,[27,28] which gives probabilities $\{p_i\}$ for the dimer model on the hexagonal lattice and the Calogero-Sutherland (CS) model.[29,30] In particular, in Sec. III C, we analytically derive Eq. (4) using a free field representation of the gas model. In Sec. IV, we numerically demonstrate the same result in the spin-1/2 *XXZ* chain.

At a certain value of R, the system undergoes a phase transition to a massive crystal phase. As we show in Secs. III D and IV, in the massive phase breaking a symmetry, S_0 is related to the ground-state degeneracy d,

$$S_0 = \log d. \tag{5}$$

At the transition point, we observe a jump in S_0, though it is slightly obscured due to finite-size effects.

As an example showing the $c=1/2$ criticality, in Sec. V, we study an Ising chain in a transverse field [Eq. (63)]. We calculate the entropies in σ^z and σ^x bases, corresponding to the RK states built from an eight-vertex model and a 2D Ising model, respectively. The extracted constants $S_0^{(z)} \simeq -0.4387$ and $S_0^{(x)} \simeq 0.2544$ at the critical point might be generic constants characterizing the $c=1/2$ CFT, although we do not have any analytical derivation of these numbers. In the symmetry-broken phase, the constant takes $S_0^{(z)} = -\log 2$ in the σ^z basis, which is interpreted as a manifestation of $\mathbb{Z}_2$ topological order in the eight-vertex RK state.

As a related quantity, in Sec. VI, we study the scaling of the largest probability $p_0 := \max p_i$. This maximum is attained by crystal states $|i_0\rangle$, e.g., by Néel states $|\uparrow\downarrow\uparrow\downarrow\ldots\rangle$ and $|\downarrow\uparrow\downarrow\uparrow\ldots\rangle$ for the *XXZ* chain in zero magnetic field. Very similarly to the entropy $S(L)$, the logarithm of p_0 has a dominant linear contribution followed by a subleading constant

$$-\log p_0 = \tilde{\alpha}L + \gamma + o(1). \tag{6}$$

For $c=1$ critical systems, our numerical results in the Dyson-Gaudin gas and the *XXZ* chain show that

$$\gamma = \log R. \tag{7}$$

This result, together with Eq. (4), gives a simple and universal way to determine the radius R from a ground-state wave function.

Here we comment on closely related works. Using boundary CFT, Hsu *et al.*[24] also studied the entanglement entropy of 2D RK wave functions for a half-cylinder. Their prediction for the constant S_0 differs from ours, although it matches our calculation for a different constant γ appearing in $-\log p_0$. A quantity similar to p_0 has also been studied by Campos Venuti *et al.*[31] in the context of fidelity, in agreement with our result [Eq. (7)].

II. CORRESPONDENCE BETWEEN SHANNON AND ENTANGLEMENT ENTROPIES

In this section, we formulate the connection between the entanglement entropy of Rokhsar-Kivelson states and the Shannon entropy of the ground states of 1D quantum models.

A. Generalized Rokhsar-Kivelson states

We start from a discrete classical (spin) model on a 2D lattice defined by Boltzmann weights $e^{-E(c)}$ for microscopic configurations c of the system. The partition function is given by

$$\mathcal{Z} = \sum_c e^{-E(c)}. \tag{8}$$

The Hilbert space of a 2D quantum system is constructed by associating a basis state $|c\rangle$ to each classical configuration c. Then, one can define a generalized RK wave function as the linear combination of all the basis states $|c\rangle$ with amplitudes given by the square roots of the classical Boltzmann weights,[21,22]

$$|RK\rangle = \frac{1}{\sqrt{\mathcal{Z}}} \sum_c e^{-(1/2)E(c)} |c\rangle. \tag{9}$$

The RK state shares the same correlations with the original classical model as long as one focuses on the diagonal correlations in the $\{|c\rangle\}$ basis. This type of state was first introduced as the ground state of the quantum dimer model on the square lattice, where $\{c\}$ are fully packed dimer coverings of the lattice. Later, the same type of states has been studied for different lattices (hexagonal,[32] triangular,[33] kagome,[34] etc.) and for a modified dimer model.[35] The RK states for the
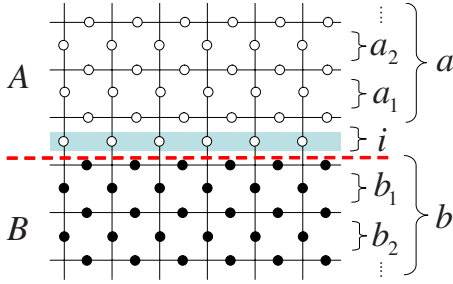
FIG. 2. (Color online) Spatial division of the square lattice into regions A and B, corresponding to the procedure in Sec. II B 1. The system is defined on a cylinder and is periodic in the horizontal direction.

eight-vertex model on the square lattice have also been studied.[36]

B. Schmidt decomposition and entanglement entropy

We divide the system into two parts, A and B, as in Fig. 1. The reduced density matrix ρ_A is obtained from a state $|\mathrm{RK}\rangle$ by tracing out the degrees of freedom in B,

$$\rho_A = \mathrm{Tr}_B |\mathrm{RK}\rangle\langle\mathrm{RK}|. \tag{10}$$

We are interested in the (von Neumann) entanglement entropy of A,

$$S^{\mathrm{vN}}(A) = -\mathrm{Tr}\,\rho_A \log \rho_A. \tag{11}$$

Here we show that the calculation of $S^{\mathrm{vN}}(A)$ for a RK state [Eq. (9)] can be recast as a fully classical calculation, provided that the boundary between A and B satisfies certain geometrical conditions. This is done by deriving a Schmidt decomposition of the RK state [Eq. (9)].

1. Case with local constraints

We first consider the case where the classical model contains certain local constraints. For simplicity, we assume that the system consists of Ising variables σ_j sitting on the bonds of the square lattice as in Fig. 2. (The same argument also applies to a model on the hexagonal lattice.) Around each site, the four Ising variables σ_j's satisfy the following constraint: if three of them are specified, the last one is uniquely determined. Dimer, six-vertex, and loop models satisfy this condition. For example, in the case of a dimer model, we assign $\sigma_j = \pm 1$ to the presence or absence of a dimer on the bond j. Then, there is strictly one bond with $\sigma_j = +1$ emanating from each site.

We define the system on a cylinder and divide it into A and B, as shown in Fig. 2. Here, all spins at the boundary belong to A. The spin configurations a and b inside A and B must agree with the configuration i at the boundary. Let $\mathcal{E}_i^A$ ($\mathcal{E}_i^B$) be a set of such a's (b's). Thanks to the local constraints, such sets share no common element,

$$\mathcal{E}_i^\Omega \cap \mathcal{E}_{i'}^\Omega = \emptyset \quad (\Omega = A, B; i \neq i'). \tag{12}$$

We assume that the classical model $E(c)$ contains only local interactions involving four bonds around each site. The energy can then be decomposed into two parts,

$$E(c) = E_A(a,i) + E_B(b,i). \tag{13}$$

The first term corresponds to all the interactions among spins in A. The second corresponds to interactions among spins in B and the boundary region. The important point is the absence of direct interaction between spins inside A and B. Thanks to this property, the Boltzmann weight of the configuration $c = (a,i,b)$ factorizes into two parts, which allows us to rewrite Eq. (9) as follows:

$$|\mathrm{RK}\rangle = \frac{1}{\sqrt{\mathcal{Z}}} \sum_i \left[\sum_{a \in \mathcal{E}_i^A} e^{-(1/2)E_A(a,i)} |a,i\rangle \right]$$
$$\times \left[\sum_{b \in \mathcal{E}_i^B} e^{-(1/2)E_B(b,i)} |b\rangle \right]. \tag{14}$$

We define normalized RK states (boundary dependent) on A and B as

$$|\mathrm{RK}_i^A\rangle := \frac{1}{\sqrt{\mathcal{Z}_i^A}} \sum_{a \in \mathcal{E}_i^A} e^{-1/2 E_A(a,i)} |a,i\rangle, \tag{15a}$$

$$|\mathrm{RK}_i^B\rangle := \frac{1}{\sqrt{\mathcal{Z}_i^B}} \sum_{b \in \mathcal{E}_i^B} e^{-1/2 E_B(b,i)} |b\rangle, \tag{15b}$$

$$\text{with } \mathcal{Z}_i^\Omega = \sum_{\omega \in \mathcal{E}_i^\Omega} e^{-E_\Omega(\omega,i)} \quad (\Omega = A, B). \tag{15c}$$

Then we arrive at the Schmidt decomposition,

$$|\mathrm{RK}\rangle = \sum_i \sqrt{p_i} |\mathrm{RK}_i^A\rangle |\mathrm{RK}_i^B\rangle, \quad \text{with } p_i := \frac{\mathcal{Z}_i^A \mathcal{Z}_i^B}{\mathcal{Z}}. \tag{16}$$

Here, the mutual orthogonality $\langle\mathrm{RK}_i^\Omega|\mathrm{RK}_{i'}^\Omega\rangle = \delta_{ii'}$ is guaranteed by Eq. (12). The reduced density matrix ρ_Ω (with $\Omega = A$ or B) is then[37]

$$\rho_\Omega = \sum_i p_i |\mathrm{RK}_i^\Omega\rangle\langle\mathrm{RK}_i^\Omega|. \tag{17}$$

Therefore, we get

$$S^{\mathrm{vN}}(A) = -\sum_i p_i \log p_i. \tag{18}$$

The entanglement entropy can thus be computed from the classical partition functions $\mathcal{Z}_i^A \mathcal{Z}_i^B$ with boundary spins fixed in a state i. Similar formulations were used in Refs. 13–16 for exact, perturbative, and/or numerical calculations of entanglement entropy in toric code, quantum eight-vertex, and quantum dimer models.

2. General case

The above discussion relies on the presence of local constraints. Without them, any configuration b is allowed in B irrespective of i, and states $\{|\mathrm{RK}_i^B\rangle\}$ defined in Eq. (15b) are not mutually orthogonal in general. Even in such a general case, one can slightly modify the model so that the entanglement entropy can be computed in the same formulation.

For simplicity, we assume that the classical model is defined on the square lattice, and a spin-S degree of freedom
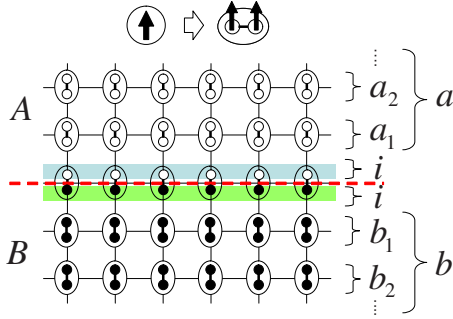
FIG. 3. (Color online) Spatial division of the square lattice, corresponding to the procedure in Sec. II B 2. Each spin of the original model is replaced by a *pair* of spins. An infinitely strong ferromagnetic interaction ensures that the two spins are always in the same state. The (new) lattice is divided in two regions, *A* and *B*, and the original sites which overlap with both regions are called "boundary" sites. The RK state admits a simple Schmidt decomposition (see text) if the only interactions between *A* and *B* take place inside the boundary region. For general short ranged interactions (not necessarily first neighbor), this condition can be achieved by choosing a sufficiently "fattened" boundary region.

lives on every site. We again assume that the energy $E(c)$ consists only of interactions between nearest-neighbor spins. As illustrated in Fig. 3, each spin is *duplicated* and an infinitely strong "ferromagnetic" interaction is added so that the two copies of the original spin are always in the same state (no spurious degrees of freedom are introduced). Then the two regions *A* and *B* are introduced in such a way that all the spin-spin interactions in $E(c)$ take place inside *A* or *B*. In other words, the only allowed couplings between *A* and *B* are the infinitely strong ferromagnetic interactions between copies of the same physical spin. If one prefers to think in terms of the original spins only (not duplicated), this amounts to saying that regions *A* and *B* are overlapping around their boundary.

In this setup, each state $|c\rangle$ can be labeled in the following way:

$$|c\rangle = |a,i\rangle \otimes |b,i\rangle. \qquad (19)$$

Here, each original spin lying at the boundary is effectively "split" and has one copy in $|a,i\rangle$ and the other in $|b,i\rangle$. The Schmidt decomposition [Eq. (16)] is then constructed using the following states:

$$|RK_i^\Omega\rangle := \frac{1}{\sqrt{\mathcal{Z}_i^\Omega}} \sum_\omega e^{-1/2E_\Omega(\omega,i)}|\omega,i\rangle, \qquad (20a)$$

with $\mathcal{Z}_i^\Omega = \sum_\omega e^{-E_\Omega(\omega,i)} \quad (\Omega = A,B). \qquad (20b)$

Here, the difference from Eq. (15) is the presence of i inside the ket $|\omega,i\rangle$ for both $\Omega=A$ and B, which ensures the mutual orthogonality of $\{|RK_i^\Omega\rangle\}$.

C. Transfer matrix calculation of the reduced density matrix spectrum

In Sec. II B 2, the spectrum $\{p_i\}$ of the reduced density matrix has been expressed in terms of the classical partition functions with spins fixed in the boundary region. In the cylindrical geometry of Fig. 1 with circumference L and height $2h$, we can relate this spectrum to the ground state of a 1D quantum spin model using the transfer matrix formalism.

Corresponding to the 2D classical model, we introduce the transfer matrix $\mathcal{T}$ in the upward direction in such a way that it connects spin configurations on neighboring "rings" winding around the cylinder (e.g., a_1 and a_2 shown in Figs. 2 and 3). The classical partition function [Eq. (8)] is then expressed as

$$\mathcal{Z} = \sum_{a_{h-1},\dots,a_1} \sum_i \sum_{b_1,\dots,b_{h-1}} \qquad (21)$$

$$\langle a_h|\mathcal{T}|a_{h-1}\rangle\cdots\langle a_2|\mathcal{T}|a_1\rangle\langle a_1|\mathcal{T}|i\rangle \qquad (22)$$

$$\times\langle i|\mathcal{T}|b_1\rangle\langle b_1|\mathcal{T}|b_2\rangle\dots\langle b_{h-1}|\mathcal{T}|b_h\rangle \qquad (23)$$

$$=\langle a_h|\mathcal{T}^{2h}|b_h\rangle. \qquad (24)$$

Here, the spin configurations, a_h and b_h, at the top and bottom edges of the cylinder are fixed. In this setup, the classical probability to find a given configuration i on the ring (boundary) is

$$p_i = \frac{1}{\mathcal{Z}}\langle a_h|\mathcal{T}^h|i\rangle\langle i|\mathcal{T}^h|b_h\rangle. \qquad (25)$$

We now consider the limit of a long cylinder $h\gg L$ so that only the dominant eigenvector $|g\rangle$ of $\mathcal{T}$ (with the largest eigenvalue m_0) contributes. Using $\mathcal{T}^h\simeq m_0^h|g\rangle\langle g|$, we get

$$p_i \simeq |\langle i|g\rangle|^2. \qquad (26)$$

If the transfer matrix is related to 1D quantum Hamiltonian $\mathcal{H}$ via $\mathcal{T}\simeq e^{-\tau\mathcal{H}}$ (with τ being a small time interval), $|g\rangle$ is the ground state of $\mathcal{H}$. Then, Eq. (26) means that the complete spectrum of the reduced density matrix ρ_A is given by the elements of the ground-state vector $|g\rangle$.

In the rest of the paper, we will make an extensive use of this property to calculate the entanglement entropy [Eq. (18)]. We study several RK states (dimer, vertex, and Ising models) defined on the infinite cylinder for relatively large values of L (maximally, $L=48$ for the dimer models and $L=32$ in the six-vertex models with no field).

D. Thermodynamic extension

The spectrum $\{p_i\}$ of the reduced density matrix ρ_A for a RK state has a simple interpretation in terms of boundary free energy of the classical model. Using Eq. (16), we get

$$-\log p_i = F_i^A + F_i^B - F, \qquad (27)$$

where $F_i^A := -\log \mathcal{Z}_i^A$ (F_i^B) is the free energy of the subsystem *A* (*B*) with its boundary with *B* (*A*) fixed in the configuration

i. Also, $F = -\log \mathcal{Z}$ is the free energy of the whole system, without any constraint on the spin configuration at the boundary between A and B. We now identify the right-hand side (rhs) of Eq. (27) as an effective energy $2E(i)$ for the boundary spins.[38] Then the entanglement entropy $S^{\text{vN}}(A)$ in Eq. (18) can be interpreted as the "thermal" entropy for the boundary spins. We push further this thermodynamic interpretation of $S^{\text{vN}}(A)$ by introducing a parameter β in order to modify the probabilities p_i,

$$p_i = e^{-2E(i)} \rightarrow p_i(\beta) = \frac{1}{Z(\beta)} e^{-\beta E(i)}, \qquad (28)$$

where $Z(\beta) = \sum_i e^{-\beta E(i)}$ is a normalization factor [with $Z(\beta=2)=1$]. Here, β plays the role of an effective inverse temperature for the boundary spins [but *a priori not* for the bulk of the classical system defined by Eq. (8)]. This allows us to generalize the entropy $S(\beta=2) = S^{\text{vN}}(A)$ to arbitrary $\beta > 0$. It can be computed through the standard thermodynamical relation $S(\beta) = (1 - \beta \partial_\beta) \log Z(\beta)$. This formulation will be useful in Sec. III. We note that a similar extension of entanglement entropy has also been discussed by Li and Haldane.[39,40]

III. FROM CRITICAL DIMER RK STATES TO DYSON-GAUDIN COULOMB GAS

In this section, we study critical dimer RK states on bipartite lattices and a related 1D classical gas model. Using the formulation of Sec. II, we compute the entanglement entropies of the dimer RK states using the dominant eigenvectors of the transfer matrices. As described in Appendixes B and C, the transfer matrices of the dimer models can be expressed as free fermion Hamiltonians, and their dominant eigenvectors are Slater determinants. In particular, for the hexagonal lattice dimer model, the resulting probabilities $\{p_i\}$ coincide with the Boltzmann weights of a 1D lattice gas interacting via a repulsive logarithmic potential (Dyson-Gaudin gas) at the inverse temperature $\beta=2$. This gas model is also related to the discretized.[41] Therefore, the entanglement entropy of the dimer RK state and the Shannon entropy of the discretized Calogero-Sutherland ground-state wave function coincide with the thermal entropy of the gas model. As we will demonstrate in Secs. III A and III B, this entropy contains a nonextensive constant contribution [Eq. (4)]. In Sec. III C, we derive it analytically using the free field representation of the gas model in the continuum limit.

A. Critical dimer RK states

We start from the RK states [Eq. (9)] constructed from the dimer models on the hexagonal and square lattices. The energy $E(c)$ takes zero for any fully packed dimer configuration c and infinity otherwise. These RK states are the ground states of quantum dimer models at special points and are known to be critical.[21,32] By associating an Ising variable $\sigma_j = \pm 1$ with the dimer occupation on each bond j, we can adopt the formulation presented in Secs. II B 1 and II C to compute the half-cylinder entanglement entropy S^{vN}.

As described in Appendixes B and C, the transfer matrices $\mathcal{T}$ of the dimer models are expressed as free fermion Hamiltonians. Their dominant eigenvectors $|g\rangle$ are Slater determinants (Fermi sea), and the weight $p_i = |\langle i|g\rangle|^2$ can be computed by evaluating a determinant. Let us focus on the hexagonal case, where a simple expression for $\{p_i\}$ is available. We here assume that L is a multiple of 6 for the sake of simplicity. A generic configuration i of the boundary will be given by a number $n \in \{0, \dots, L\}$ of fermions living on the vertical edges of the boundary and their positions,

$$0 \leq \alpha_1 < \dots < \alpha_n \leq L - 1. \qquad (29)$$

It is also shown in Appendix B that, in the limit $h \gg L$, the only nonzero probabilities correspond to $n = 2L/3$ fermions and are given by a Vandermonde determinant, which simplifies into

$$p_i = \frac{1}{L^n} \prod_{1 \leq j < j' \leq n} 4 \sin^2\left(\frac{\pi}{L}(\alpha_j - \alpha_{j'})\right). \qquad (30)$$

This equation is invariant under $n \rightarrow L - n$. Therefore it is easier to compute it with $n = L/3$ fermions instead of $n = 2L/3$. As we will see in Sec. III B, these probabilities coincide with the Boltzmann weights of a 1D lattice gas. Note that the present calculation is done without any constraint on the configurations, a_h and b_h, at the top and bottom of the cylinder. The number n of fermions leading to nonzero probabilities can be controlled by imposing certain boundary conditions.

Figure 4 shows the scaling of the entanglement entropy $S(L)$ for both the hexagonal and square cases. Here, in the square case, the weight p_i is computed by numerically evaluating the determinant in Eq. (C19). In the hexagonal case, we examine different fermion densities $\rho = n/L$ (or equivalently flux and/or winding sectors in the dimer language). In every case, the scaling of $S(L)$ appears to be approximately linear in L. The slope is nonuniversal, as expected, and depends on the details of the system. The most interesting result is the existence of a finite constant S_0. By fitting the large-L values by $S(L) = \alpha L + S_0 + b/L$, we find $S_0 = -0.500 \pm 0.002$ in all cases. These results suggest that $S_0 = -1/2$ is a universal number for this family of RK wave functions.

B. Dyson-Gaudin gas on a circle

We consider a system of n charges $Q = -1$, living on a periodic one-dimensional lattice with L sites as in Fig. 5. These charges interact via a 2D Coulomb repulsive potential equal to minus the logarithm of their mutual distance. For convenience, we add a uniform background of L charges $Q = +1/2$ located on each site of the lattice. A configuration of the system will be determined by the positions $1 \leq \alpha_1 < \alpha_2 < \dots < \alpha_n \leq L$ of the charges. Two charges cannot occupy the same site. The energy of a given configuration i is

Dimers on the hexagonal and square lattices
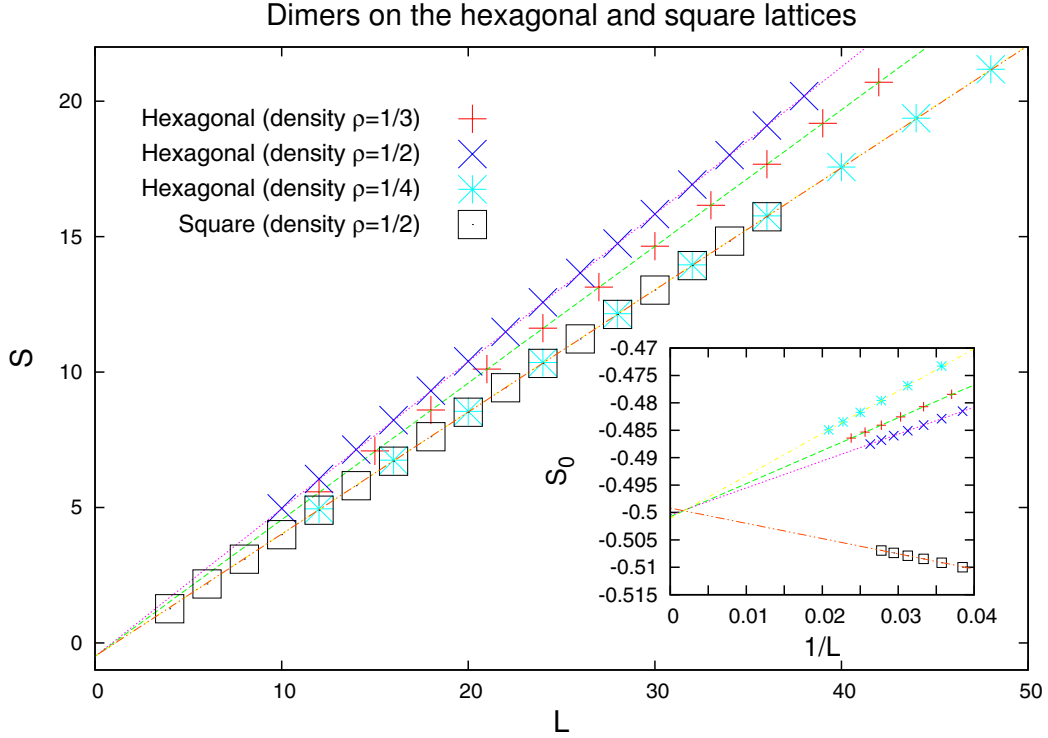
FIG. 4. (Color online) Entanglement entropy of RK states corresponding to dimer models on the hexagonal lattice (with fermion densities $\rho=1/4, 1/3, 1/2$) and the square lattice (with $\rho=1/2$). In all cases, the entropy scales as $S \simeq \alpha L + S_0 + b/L$ with $S_0 = -0.500(2)$. The inset shows S_0', the subleading constant computed this time from a linear fit $S \simeq a'L + S_0'$ on the interval $[12, L]$ as a function of $1/L$. The convergence toward $-0.500(1)$ can be seen.

$$E(i) = - \sum_{1 \le j < j' \le n} \log\left|e^{(2\pi i/L)\alpha_j} - e^{(2\pi i/L)\alpha_{j'}}\right| + \frac{n}{2}\log L, \tag{31}$$

where the second term comes from the interaction of each charge with the background. This may be viewed as a discretized version of the Dyson gas[27] and has been studied by Gaudin[28] (hence we name it the Dyson-Gaudin gas). As in Sec. III A, the "particle-hole" symmetry $n \to L-n$ is worth noticing. The classical 1D partition function is given by $Z(\beta) = \Sigma_i e^{-\beta E(i)}$ for an inverse temperature β, and the classical entropy can be calculated from it,

$$S(\beta) = \left(1 - \beta\frac{\partial}{\partial\beta}\right)\log Z(\beta). \tag{32}$$

Gaudin[28] evaluated the partition function exactly in the special cases where $\beta = 2\lambda$ with λ as an integer and $\lambda < L/(n-1)$,[1]

$$Z_n^{(L)}(2\lambda) = \frac{(n\lambda)!}{n! \, L^{n(\lambda-1)}(\lambda!)^n}. \tag{33}$$

The probabilities $\{p_i\}$ in Eq. (30) calculated for the hexagonal lattice dimer model coincide exactly with the Boltzmann weights of the Dyson-Gaudin gas model with $\beta = 2$: $p_i = e^{-2E(i)}$.

Hence the entanglement entropy for this dimer model corresponds to the thermal entropy $S(\beta=2)$ of the gas model. Note that $Z(\beta=2) = 1$ if we set $\lambda = 1$ in Eq. (33) because p_i in

Eq. (30) is already normalized. In the spirit of Sec. II D, we can generalize the entanglement entropy by changing the inverse temperature β. We define $p_i(\beta) = p_i^{\beta/2}/Z(\beta) = e^{-\beta E_i}/Z(\beta)$, and the associated Shannon entropy

$$S(\beta) = -\sum_i p_i(\beta)\log p_i(\beta) \tag{34}$$

coincides with the thermal entropy [Eq. (32)] of the gas model. Notice that Gaudin's solution (33) cannot be used to compute the entropy $S(\beta)$ because it is valid only for special values of β. Instead, we compute $S(\beta)$ numerically by explicitly summing over all the configurations.
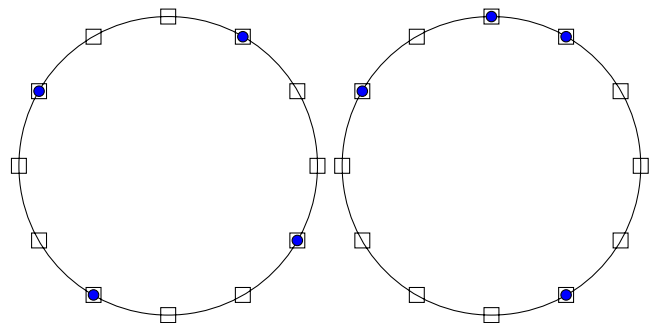
FIG. 5. (Color online) System of $n=4$ charges $Q=-1$ on a circle with $L=12$ sites. The left shows the configuration with highest probability (degeneracy: 3) and the right shows a random configuration. On each site, a "background" charge $Q=+1/2$ is added.

Dimers on the hexagonal lattice : subleading constant S_0 in the entropy
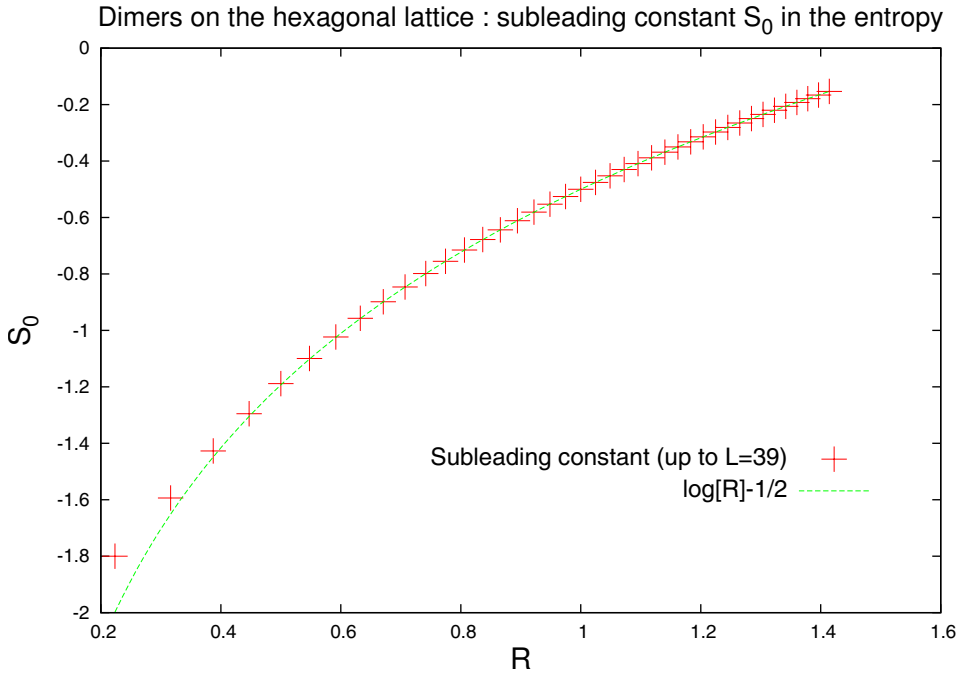
FIG. 6. (Color online) The subleading constant S_0 in the thermal entropy of the Dyson-Gaudin gas with density $\rho = 1/3$ as a function of $R = \sqrt{\beta/2}$. At $\beta = 2$, this coincides with the constant part in the entanglement entropy of the hexagonal dimer RK state shown in Fig. 4. The data well obey Eq. (36).

Here we mention the connections with other models. The Dyson gas model emerges in the weights $|\langle i|g\rangle|^2$ of the Jastrow-type ground-state wave function of the CS model.[29,30] The inverse temperature β of the gas model is related to the coupling constant of the CS model. The CS model is described as a Tomonaga-Luttinger liquid at low energies. According to a spectral analysis of the CS model,[42] the boson radius R is related to β as

$$R = \sqrt{\frac{\beta}{2}}. \tag{35}$$

This allows us to control R simply by changing β. This relation will also be justified from a different viewpoint in Sec. III C. The Haldane-Shastry model[43,44] is a discretized version of the CS model, and its Jastrow ground state (Gutzwiller-projected Fermi wave function) has the weights exactly obeying the Dyson-Gaudin gas with $\beta = 4$. This model has $R = \sqrt{2}$ because of the SU(2) symmetry in consistency with Eq. (35). Note also that the same wave function is known to be an extremely good ansatz for the ground state of the Heisenberg chain.

Now we analyze the thermal entropy $S(\beta)$ of the gas model. We extract the nonextensive constant contribution S_0 as in Fig. 4 and plot it as a function of $R = \sqrt{\beta/2}$ in Fig. 6. We find that the data agree well with a simple relation

$$S_0 = \log R - \frac{1}{2}. \tag{36}$$

This expression is derived analytically in Sec. III C. It should be noted that the subleading constant [Eq. (36)] is increasing with β, contrary to the total entropy, which is decreasing with β, as should be the case in classical thermodynamics.

C. Free bosonic field

In this section, we obtain the expression of the entropy S_0 using a field-theoretical approach. Our goals are to obtain a

continuous expression for the partition function of the gas studied in Sec. VII and deduce from it the expression of the entropy.

We consider a continuous distribution, $\rho(\theta)$, of electric charges on the unit circle. The expression of the electrostatic energy [Eq. (31)] is given by

$$E = -\frac{1}{2} \int_0^{2\pi} \rho(\theta) d\theta \int_0^{2\pi} \rho(\theta') d\theta' \, \log \left| 2 \sin\left(\frac{\theta - \theta'}{2} \right) \right|. \tag{37}$$

We define a field $\phi(\theta)$ measuring the amount of charge in the interval $[0, \theta]$ in units of 2π,

$$\phi(\theta) = 2\pi \int_0^\theta \rho(\sigma) d\sigma. \tag{38}$$

By performing partial integrations twice, the energy is rewritten as

$$E[\phi] = \frac{1}{64\pi^2} \int_0^{2\pi} d\theta \int_0^{2\pi} d\theta' \left(\frac{\phi(\theta) - \phi(\theta')}{\sin\left(\frac{\theta - \theta'}{2} \right)} \right)^2. \tag{39}$$

Since the functional integration is over $\rho = \phi'$, the zero mode of ϕ is unphysical and should be discarded [it can be removed by adding an appropriate constant to Eq. (38)]. By expanding the field ϕ over modes,

$$\phi = 2\pi \sum_{m \geq 1} (x_m e^{im\theta} + \bar{x}_m e^{-im\theta}), \tag{40}$$

the energy [Eq. (39)] reduces to

$$E = \frac{(2\pi)^2}{2} \sum_{m \geq 1} m|x_m|^2. \tag{41}$$

Integrating the Boltzmann weight $e^{-\beta E}$ over the modes $dx_m d\bar{x}_m$, we obtain the partition function Z_{sphere} of the gas,

$$Z_{\text{sphere}} = \prod_{m \geq 1} \frac{2}{2\pi\beta m}. \tag{42}$$

To find possible universal contributions to the corresponding free energy, this expression of course needs to be regularized. Following Nahm,[45] we regularize the measure $dx_m d\bar{x}_m$ to take into account the finiteness of the number of states. We set $|x_m| = \rho_m$ and take the measure to be $d(2\pi[\rho_m^2]^{f(m/\Lambda)})$, where $f(x) = 1$ in the interval $[0, 1]$ and decreases to $f(\infty) = 0$ sufficiently fast. We obtain

$$Z_{\text{sphere}} = \prod_{m=1}^{\infty} \left(\frac{1}{\pi m\beta}\right)^{f(m/\Lambda)} \Gamma[1 + f(m/\Lambda)]. \tag{43}$$

The Euler-MacLaurin formula yields

$$\prod_{m=1}^{\infty} \left(\frac{1}{\pi\beta}\right)^{f(m/\Lambda)} \Gamma\left[1 + f\left(\frac{m}{\Lambda}\right)\right] = \sqrt{\pi\beta} \exp\left[\Lambda \int_0^\infty g_\beta(x)dx\right]$$
$$\times [1 + o(1)],$$

$$g_\beta(x) = \log \Gamma[1 + f(x)] - \log(\pi\beta)f(x). \tag{44}$$

Here we decompose f into the sum of a step function on $[0, 1]$ and a function vanishing on $[0, 1]$,

$$\prod_{m=1}^{\infty} \left(\frac{1}{m}\right)^{f(m/\Lambda)} = \frac{1}{\sqrt{2\pi}} \exp\left[-\Lambda \int_0^\infty \log(\Lambda x)f(x)dx\right] [1 + o(1)], \tag{45}$$

where we have used the Stirling formula on the term corresponding to the step function and the Euler-MacLaurin formula on the other one. Putting everything together,

$$Z_{\text{sphere}} = \sqrt{\frac{\beta}{2}} \exp\left\{\Lambda \int_0^\infty dx \log \Gamma[1 + f(x)]\right.$$
$$\left. - \log(\pi\beta\Lambda x)f(x)\right\} [1 + o(1)]. \tag{46}$$

The regularized partition function is obtained after removing the exponential factor, $\Lambda^{-a\Lambda}\mu^\Lambda$, which can be thought as the "extensive" part

$$Z_{\text{sphere}} = \sqrt{\frac{\beta}{2}}. \tag{47}$$

This result is simply equal to the ζ regularization of Eq. (42). In this derivation, the normalization of the integration measure over the modes is adjusted so that $Z_{\text{sphere}} = 1$ at $\beta = 2$, in agreement with our microscopic definition of the partition function, $Z_{\text{sphere}}(\beta) = \Sigma_i p_i^{\beta/2}$, in the discrete model. From this expression, we deduce the thermal entropy,

$$S_0 = \frac{1}{2}\log\left(\frac{\beta}{2}\right) - \frac{1}{2}, \tag{48}$$

in agreement with our numerical result in Fig. 6.

Alternatively, we can normalize the field ϕ differently so as to include the inverse temperature β in its definition. We introduce a radius R and set $\beta = 2R^2$. The field ϕ is now defined mod $2\pi R$. We can extend its range of definition by requiring it to be a harmonic function on the unit disk Ω and express the energy as a Dirichlet integral,

$$\frac{\beta}{2}E = \frac{1}{4\pi} \int \int_\Omega dz d\bar{z} \partial_z \phi \partial_{\bar{z}} \phi, \tag{49}$$

where $z = x + iy$. This coincides with the action [Eq. (3)] except that the range of integration is limited to the unit disk Ω.

One can view Eq. (49) as the action of a closed string[46] propagating on a circle of radius R with a Regge slope $\alpha' = 2$. Now, if we include the center of mass (zero mode) into the definition of ϕ, we see that the regularized measure $[d\phi]$ becomes *invariant* under rescaling of the field, so that we can also take the field defining the measure to be defined mod $2\pi R$. The partition function Z_{sphere} of the electrostatic gas is obtained by sewing together two disks to form a sphere and is given by the partition function of a closed string propagating on a circle of radius R. Proceeding in this way, the oscillators do not contribute and it reduces to the center of mass integral,

$$Z_{\text{sphere}} = R, \tag{50}$$

in agreement with Eq. (47).

To understand this result, consider a closed string $\phi(\sigma, T)$ propagating in the Euclidean time T. Its partition function on the cylinder $[0, 2\pi] \times [0, T]$ with boundary fields equal to $\phi_{1,2}$ defines the propagator $Z(\phi_1, \phi_2)$. We evaluate the torus partition function Z_{torus} by taking the trace of the propagator over $\phi = \phi_1 = \phi_2$,

$$Z_{\text{torus}} = \int [d\phi] Z(\phi, \phi). \tag{51}$$

If we decompose the field ϕ into the sum of a harmonic function equal to ϕ_1, ϕ_2 at the two boundaries and a field vanishing at the boundaries, we factorize the propagator into two pieces: a classical one equal to $e^{-(\beta/2)E(\phi_1)-(\beta/2)E(\phi_2)}$ in the limit of large T and the partition function Z_{00} with Dirichlet boundary conditions. Thus, in the limit of large T, $Z_{\text{torus}} = Z_{\text{sphere}}Z_{00}$. But $Z_{00}/Z_{\text{torus}} = 1/R$ is the stationary probability distribution of the center of mass of the string diffusing on a circle of radius R and the result [Eq. (50)] follows. This formulation has the advantage to be easily generalizable to a closed surface of characteristic χ,

$$Z_\chi = R^{\chi/2}. \tag{52}$$

We expect this formula also to apply to the case of open boundary conditions with suitable chiral boundary conditions.

Let us mention that Gaudin's partition function [Eq. (33)] has the same asymptotic expression as Z_{sphere} in Eq. (42) if we remove the nonuniversal extensive part. Indeed, by tak-

Subleading constant in log(Z) : transition towards a cristal state
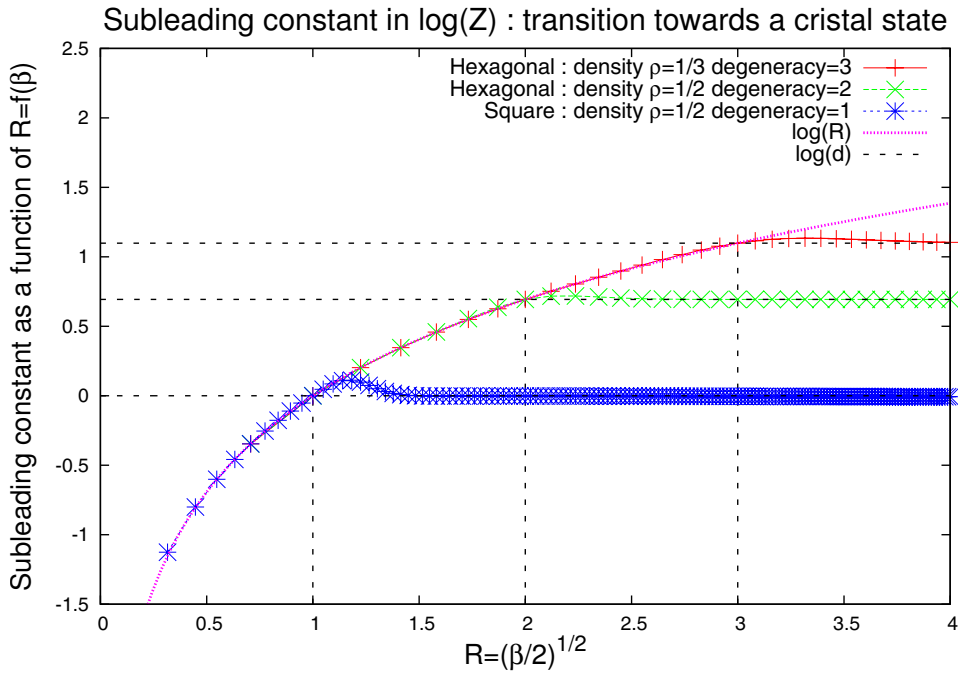
FIG. 7. (Color online) Liquid-crystal transitions induced by the boundary temperature β^{-1} in the dimer models. Here, the subleading constant C in $\log Z$ is shown. The critical radius is $R_c = d$ ($\beta_c = 2d^2$), where d is the degeneracy of the ground state. The constant C is expected to obey Eq. (55). The discrepancy slightly after R_c is very likely due to finite-size effects.

ing $n \to \infty$ while keeping $\rho = n/L$ constant, Stirling's formula $n! \simeq \sqrt{2\pi n}(n/e)^n$ applied to Eq. (33) gives

$$Z_n^{(L)}(2\lambda) = \mu(\lambda)^n R, \quad \text{with} \quad \mu(\lambda) = \frac{\rho^{\lambda-1}\lambda^\lambda e^{\lambda-1}}{\lambda!}. \quad (53)$$

Gaudin's formula (33) is only valid at integer values of λ and we cannot use it to evaluate the entropy. However, the denominator factor $L^{(\lambda-1)n}$ in Eq. (33) may be viewed as a regularization of the Dyson partition function,[27,47] where L plays the same role as Λ defined above, and the entropy also derives from the Dyson gas partition function.

The compactification radius of the (continuum) CS ground state[29,30] is known to be $R = \sqrt{(\lambda = \beta/2)}$ from Ref. 42. On the other hand, our numerics on the *discretized* version of the CS wave function indicate that the entropy constant is equal (within our numerical accuracy) to $S_0 = \log(\sqrt{\beta/2}) - 1/2$. From the analytical derivations presented above, this entropy constant must be related to the boson radius. We therefore conclude that the discretized CS state has long-distance properties described by the same boson compactification radius as the original continuum CS wave function. It is interesting to notice that this identification has been made through the ground-state structure of the CS model, i.e., without relying on the spectral properties unlike preceding approaches.[42]

D. Phase transition toward a crystal state

The numerical results of Fig. 6 show that for not too large values of β, the nonextensive contribution to the entropy is given by $S_0 = \log R - 1/2$. As should be clear from Sec. III C, this can only be true if the system is described by a massless (but compactified) free field. But for sufficiently large β, the system undergoes a transition to a crystal state with spontaneous translation symmetry breaking. A simple way to understand that such a crystal is expected at large β is to notice

that for $\beta \to \infty$, only the particle configurations i for which the (original) probability p_i is maximum survive. For a particle density $1/d$, this selects d periodic configurations with equally spaced particles (see the left panel in Fig. 5). Adding fluctuations around these regular configurations will add *extensive* contributions to $S(L)$ while keeping the subleading constant

$$S_0 = \log d \quad (54)$$

stable in a crystal phase with a d-fold spontaneous symmetry breaking. Due to some finite-size effects, it turns out that the liquid-crystal transition is easier to see in the nonextensive part C of $\log Z$ (rather than that of S). The data displayed in Fig. 7 are consistent with

$$C = \begin{cases} \log R, & R \leq R_c = d \\ \log d, & R \geq R_c = d. \end{cases} \quad (55)$$

Using $S_0 = (1 - \frac{R}{2}\partial_R)C$, we can recover the subleading term S_0 in the entropy,

$$S_0 = \begin{cases} \log R - 1/2, & R < R_c = d \\ \log d, & R > R_c = d. \end{cases} \quad (56)$$

It should be noted that the transition is only visible on the subleading terms of S and $\log Z$.

The crystallization can also be understood from a free field point of view. Let us perturb the action [Eq. (3)] by a d-fold symmetry breaking *boundary* field,

$$Z_{h_d} = \left\langle \exp\left[h_d \int_0^{2\pi} \cos(d\phi)d\theta \right] \right\rangle_{\text{sphere}}, \quad (57)$$

where the integral is taken over the equator of the sphere. In a spin wave approximation, the anomalous dimension of the field h_d is
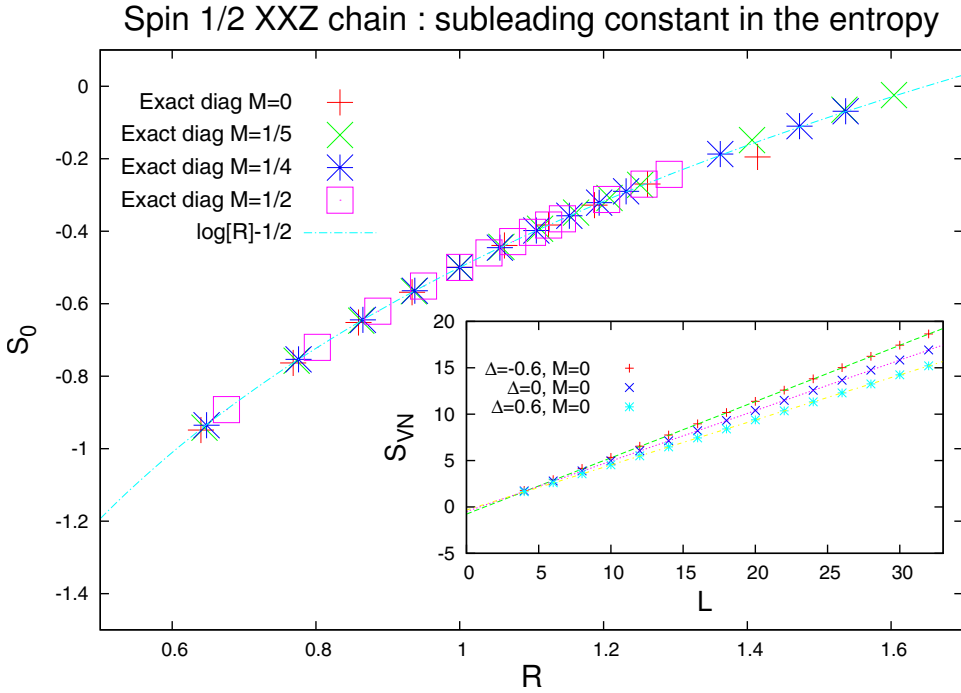
FIG. 8. (Color online) The subleading constant S_0 in the entropy S extracted from the critical ground state of the *XXZ* chain [Eq. (59)]. The examined values of Δ range from -0.8 to 1 for $M = 0$ and from -0.8 to 8 for $M = 1/5$, 1/4, and 1/2. The inset shows the fitting of the data with the scaling form $S = \alpha L + S_0 + b/L$. The constant S_0 well obeys the proposed universal formula $\log R - \frac{1}{2}$. Close to the isotropic point ($\Delta = 1$ and $M = 0$) with $R = \sqrt{2}$, a small discrepancy from the proposed formula can be seen, which is very likely due to stronger finite-size effect around this point.

$$x_d = 1 - \frac{d^2}{R^2}. \qquad (58)$$

Thus, the perturbation becomes relevant when $R \geq d$ in agreement with our observations (Fig. 7).

This transition is completely analogous to the localization transition of a macroscopic degree of freedom coupled to a dissipative environment in presence of a periodic potential.[48] In this context, the inverse temperature $\beta = 2R^2$ is a friction coefficient. A similar transition is observed in the *XXZ* chain (see Sec. IV) but at a *different* value of the compactification radius ($R = \sqrt{2}$), compatible with the bulk roughening transition of the six-vertex model.

IV. SPIN-1/2 *XXZ* CHAIN AND SIX-VERTEX RK STATES

In this section, we consider the Shannon entropy [Eq. (1)] defined from the ground state $|\psi\rangle$ of the spin-$\frac{1}{2}$ *XXZ* chain,

$$\mathcal{H} = \sum_j (\sigma_j^x \sigma_{j+1}^x + \sigma_j^y \sigma_{j+1}^y + \Delta \sigma_j^z \sigma_{j+1}^z) - h \sum_j \sigma_j^z. \quad (59)$$

This Hamiltonian is related to the transfer matrix of the classical six-vertex model on the square lattice.[49,50] Thus, using the argument of Sec. II, the Shannon entropy S here can also be interpreted as the entanglement entropy of the RK state built from this vertex model. Since the magnetization per site $M = \frac{1}{L} \sum_i \sigma_i^z$ is a conserved quantity, we can work in a sector with fixed M. We calculate the ground state of $\mathcal{H}$ for finite periodic chains using Lanczos diagonalization (up to $L = 32$ for $M = 0$ and $L = 40$ for $M = 1/2$) and evaluate the Shannon entropy S from it.

We first focus on the $c = 1$ Tomonaga-Luttinger liquid phase extending over a wide region in $\Delta > -1$. The boson radius R depends on Δ and M (see Refs. 51 and 52 for details). When $M = 0$, R is related to Δ via a simple relation

$$R = \sqrt{2 - \frac{2}{\pi} \arccos \Delta}, \quad -1 < \Delta \leq 1. \quad (60)$$

When $M \neq 0$, R can be determined numerically by solving the integral equations obtained from the Bethe-ansatz method.[52–54] We set M at simple fractions 0, 1/5, 1/4, and 1/2 so that we can examine the dependence on the system size L. As in the critical dimer models studied in Sec. III D, the entropy S well obeys the scaling form $S \simeq \alpha L + S_0 + b/L$. The subleading constant S_0 obtained by fitting the data is plotted as a function of R in Fig. 8, which shows a remarkable agreement with

$$S_0 = \log R - \frac{1}{2}. \qquad (61)$$

When increasing Δ at $M = 0$, the system undergoes a Kosterlitz-Thouless transition at $\Delta = 1$ from the critical phase to a massive Néel phase with doubly-degenerate ground states. In a finite-size system, the double degeneracy in the Néel phase is slightly split, and the ground state can be approximated by a macroscopic superposition of ordered states. When $\Delta \to \infty$, such a state is given by

$$|g\rangle = \frac{1}{\sqrt{2}}(|\uparrow \downarrow \ldots\rangle + |\downarrow \uparrow \ldots\rangle). \qquad (62)$$

This state gives $S = S_0 = \log 2$. As in the discussion of Sec. III D, one can expect that quantum fluctuations around state (62) occurring in $\Delta < \infty$ produce only extensive contributions and that the constant $S_0 = \log 2$ is stable in the massive phase $\Delta > 1$. Our numerical result for S_0 is presented in Fig. 9. The data show deviation from $\log 2$ when decreasing Δ, but it is likely due to finite-size effects. The peak and dip seen in the figure move to the left as we use larger L's for extracting S_0. In the thermodynamic limit, we expect a jump from $S_0 = \log \sqrt{2} - 1/2$ to $S_0 = \log 2$ at the transition point $\Delta = 1$.

XXZ chain : phase transition for the subleading term in the entropy
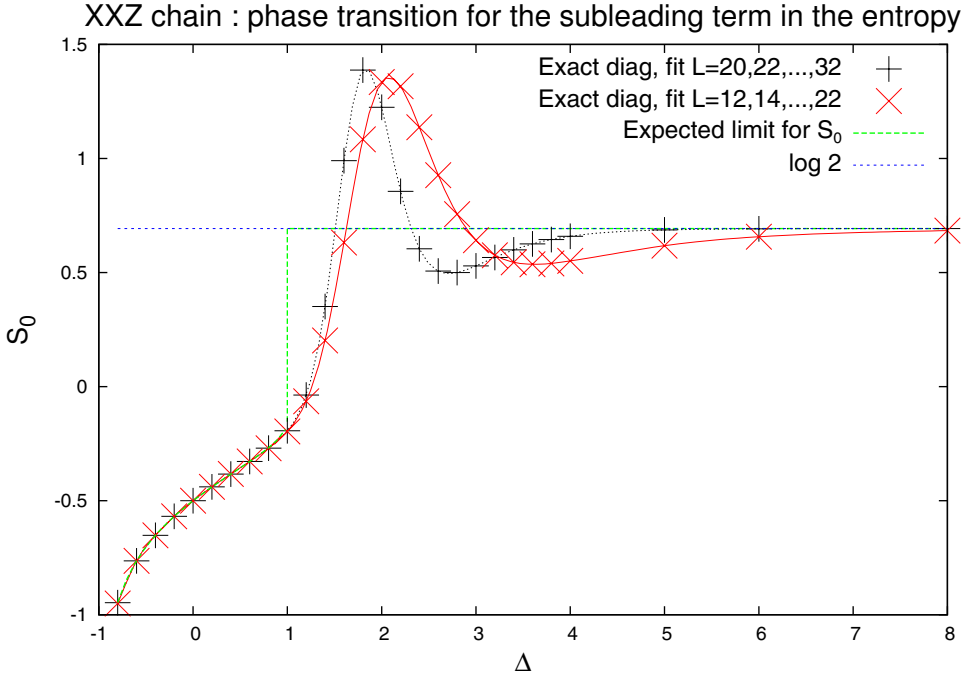
FIG. 9. (Color online) The constant part S_0 of the entropy and the phase transition in the *XXZ* chain at $M=0$. In the thermodynamical limit, we expect S_0 to be $S_0 = \log R(\Delta) - 1/2$ for $-1 < \Delta \le 1$ and $S_0 = \log 2$ for $\Delta > 1$.

Finally, we note that the *XXZ* chain with $\Delta = 1/2$ and $h = 0$ corresponds to the so-called ice model,[49,50] where all the configurations satisfying the ice rule (two in and two out around every vertex) occur with equal probabilities. The RK state built from the ice model has been studied for the spin and fermionic models on the checkerboard lattice.[55,56] The result in this section shows that the half-cylinder entanglement entropy of this state has a subleading constant $S_0 = \log\sqrt{4/3} - 1/2$.

V. ISING CHAIN IN A TRANSVERSE FIELD

As an example showing a $c=1/2$ critical point, in this section, we study an Ising chain in a transverse field,

$$\mathcal{H} = -\mu \sum_{j=0}^{L-1} \sigma_j^x \sigma_{j+1}^x - \sum_{j=0}^{L-1} \sigma_j^z. \qquad (63)$$

This model is related to two types of 2D classical models depending on which basis we work with.[50] In the σ^x basis, we have a 2D Ising model,

$$E = -\sum_{\langle jj' \rangle} \sigma_j^x \sigma_{j'}^x, \qquad (64)$$

where jj' runs over all the nearest-neighbor pairs of sites on the square lattice. This model shows a low-temperature ordered phase and a high-temperature paramagnetic phase. On the other hand, in the σ^z basis, we have an eight-vertex model of special type. The spins σ_j^z are placed on the bonds of the square lattice and satisfy local constraints; the product of four spins around each site must be even,

$$\prod_{j \in +} \sigma_j^z = +1. \qquad (65)$$

Then the four spins can take eight states out of 2^4 possibilities, hence it is named eight vertex. The energy is given by

$$E = -\sum_j \sigma_j^z. \qquad (66)$$

It is useful to introduce a loop representation of the configurations. We regard the lowest-energy state ($\sigma_j^z = +1$ for all j) as the "vacuum" and place a loop element on every bond j with $\sigma_j^z = -1$. Then only closed loops are formed because of the local constraints [Eq. (65)]. Equation (66) means that the energy cost to generate loops is proportional to their total length. At low temperatures, the system contains only small loops and is dominated by the vacuum ("small-loop" phase). At high temperatures, the formations of large loops are allowed and the system gets disordered ("large-loop" phase). The correspondence among quantum and classical models is shown in Table I, together with our results for the entropy which we present below.

Here we consider the Shannon entropies, $S^{(z)}$ and $S^{(x)}$, defined in the σ^z and σ^x bases, respectively. These correspond to the half-cylinder entanglement entropies of the RK states built from the eight-vertex model and the 2D Ising model, respectively (notice that for the latter, one needs to modify the model slightly in order to simplify the calculation, as presented in Sec. II B 2). The RK state constructed from the eight-vertex model [Eq. (66)] in the large-loop phase is particularly interesting because it possesses topological order. Such a state has been studied as the ground state of a quantum eight-vertex model[16,36] (also known as an extended toric code model[15]).

As is well known, Hamiltonian (63) reduces to a fermionic quadratic form using the Jordan-Wigner transformation. It can then be diagonalized using the Bogoliubov transformation (see Appendix E). The weight $|\langle i|g\rangle|^2$ of each spin configuration $|i\rangle$ in the σ^z basis can be obtained by calculating a Pfaffian, and $S^{(z)}(L)$ is computed numerically by summing over all the 2^L configurations.
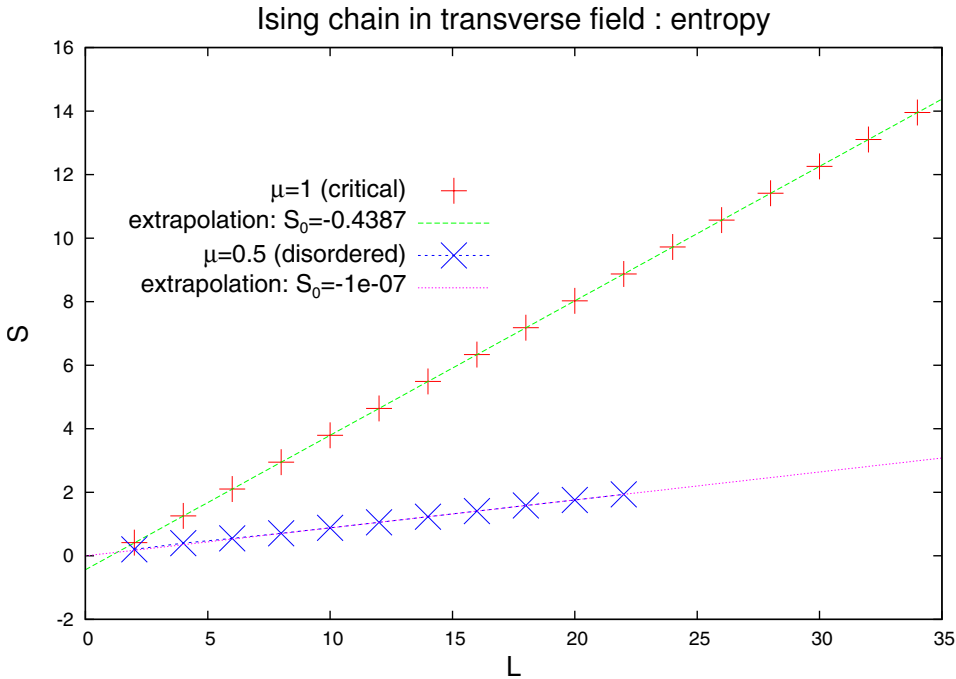
FIG. 10. (Color online) Entropy $S^{(z)}$ computed from the ground state of an Ising chain in a transverse field up to $L=36$ spins. The data for $\mu=1$ (critical point) are well reproduced by $S^{(z)} \simeq \alpha L + S_0^{(z)} + \delta/L$ with $S_0^{(z)} \simeq -0.4387(1)$ (determined from a fit to the last three points $L=32, 34, 36$). For $\mu=0.5$ in the disordered phase, the constant is very close to zero (a fit to the three points $L=18, 20, 22$ gives $|S_0^{(z)}| \leq 10^{-6}$).

The scalings of $S^{(z)}(L)$ are shown in Fig. 10. We again observe nice agreement with a linear scaling $S^{(z)}(L) = \alpha L + S_0^{(z)}$ both in the critical and massive cases. At the critical point ($\mu=1$), we find the subleading constant in the entropy to be

$$S_0^{(z)} = -0.4387 \pm 0.0001. \qquad (67)$$

Figure 11 shows the constant part $S_0^{(z)}$ as a function of the coupling constant μ. Away from the critical point, the constant is stable at certain values: $S_0^{(z)} = 0$ in the disordered phase ($\mu < 1$) and $S_0^{(z)} = -\log 2$ in the ferromagnetic phase ($\mu > 1$). Deviations from these values near the critical point are likely due to finite-size effects because they decay as we increase the system size. These values can be understood by considering two limits. In the limit $\mu=0$, the ground-state wave function is $|g\rangle = |\uparrow\uparrow \dots \uparrow\rangle_z$ and the entropy $S^{(z)}$ is zero. In the limit $\mu \to \infty$, the wave function is

$$|g\rangle = \frac{1}{\sqrt{2}}(|\uparrow\uparrow \dots \uparrow\rangle_x + |\downarrow\downarrow \dots \downarrow\rangle_x)$$

$$= \frac{1}{\sqrt{2^{L-1}}} \sum_{\sigma_1=\uparrow,\downarrow} \dots \sum_{\substack{\sigma_L=\uparrow,\downarrow \\ \Pi\, \sigma_j^z=+1}} |\sigma_1\rangle_z \otimes \dots \otimes |\sigma_L\rangle_z, \qquad (68)$$

where all the configurations have an even number of up spins in the σ^z basis. Therefore, the entropy is

$$S^{(z)}(L) = (L-1)\log 2. \qquad (69)$$

As explained in Secs. III D and IV, we expect that quantum fluctuations around these limits produce only extensive contributions and keep the subleading constants stable.

It is useful to interpret these results in terms of the eight-vertex RK state. When the temperature of the eight-vertex model is set to infinity, the corresponding RK state is an equal-amplitude superposition of all the loop configurations.

This is the ground state of Kitaev's toric code model.[57] Using the method in Ref. 13, the half-cylinder entanglement entropy is shown to scale exactly as Eq. (69), and the constant part $S_0^{(z)} = -\log 2$ can be interpreted as the topological entropy[9,10] associated with $\mathbb{Z}_2$ topological order. Microscopically, $-\log 2$ comes from the fact that in any configuration, the loops cross an *even* number of time with the boundary separating the two half-cylinders. The result in Fig. 11 therefore demonstrates the stability of this topological entropy for the half-cylinder geometry in the entire large-loop phase. The jump in the entropy around $\mu=1$ is interpreted as a break-down of topological order. We comment that the stability of topological entropy has also been studied on the same wave function for the disk and annulus geometries in Refs. 15 and 16.
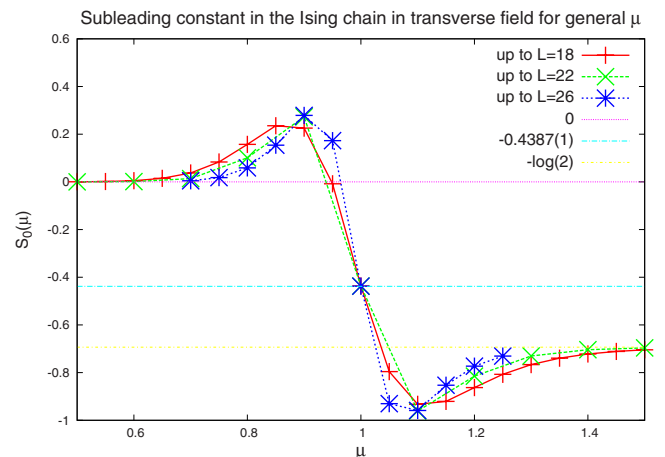
FIG. 11. (Color online) Subleading constant $S_0^{(z)}$ extracted from the entropy $S^{(z)}(L)$ in an Ising chain in a transverse field for different values of μ.

Subleading constant in the entropy for the Ising chain as a function of β
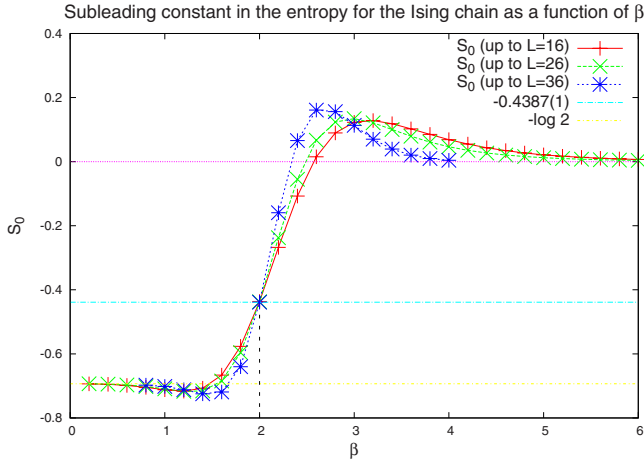
FIG. 12. (Color online) Subleading constant $S_0^{(z)}(\beta)$ extracted from the entropy $S^{(z)}(L; \beta)$ in an Ising chain in a transverse field at the critical point $\mu = 1$. The inverse temperature β is introduced as explained in Sec. II D.

We move on to the entropy $S^{(x)}$ in the σ^x basis. It can be related to $S^{(z)}$ using the Kramers-Wannier duality transformation,[58]

$$\sigma_j^z \to \tilde{\sigma}_{j-1}^x \tilde{\sigma}_j^x, \quad \sigma_j^x \sigma_{j+1}^x \to \tilde{\sigma}_j^z, \qquad (70)$$

by which $\mathcal{H}(\mu)$ is related to $\mathcal{H}(1/\mu)$. Here, $\tilde{\sigma}_j^z = -1$ is identified with a domain wall between σ_j^x and σ_{j+1}^x. Taking into account the two-to-one correspondence between σ^x and $\tilde{\sigma}^z$ configurations, one can show

$$S^{(x)}(\mu) = S^{(z)}(1/\mu) + \log 2. \qquad (71)$$

Hence we obtain the results summarized in Table I. Now we have a positive constant $S_0^{(x)} = \log 2$ in the ordered phase $\mu > 1$. This is a consequence of the macroscopic superposition of two ordered states, as discussed for the ordered phase of the XXZ chain in Sec. IV.

We have obtained two constants $S_0^{(z)} = -0.4387(1)$ and $S_0^{(x)} = S_0^{(z)} + \log 2 = 0.2544(1)$ at the critical point, depending on the choice of basis. We believe that these are generic

constants characterizing the $c = 1/2$ criticality, although at present we do not have any analytical derivation of these numbers.

We can also introduce a temperature β^{-1} for the entropy $S^{(z)}$ as described in Sec. II D. The constant part $S_0^{(z)}(\beta)$ extracted by fitting $S^{(z)}(L; \beta)$ with a linear scaling changes rapidly around $\beta = 2$ (see Fig. 12). It seems reasonable to conjecture that $S_0^{(z)}(\beta)$ becomes a step function in the thermodynamic limit: $S_0^{(z)}(\beta) = -\log 2$ for $\beta < 2$ and $S_0^{(z)}(\beta) = 0$ for $\beta > 2$. If confirmed, this result would suggest that increasing β has a role similar to decreasing μ, i.e., taking the system away from its critical point. In the $c = 1$ case, $S_0(\beta)$ was a smooth function of β (see Figs. 6–8). Therefore, it looks like introducing β has a qualitatively different effect, depending on the nature of the critical theory.

Note that there are several directions in which to extend the Ising model. One possibility is to study the q-state Potts model or the restricted solid-on-solid (RSOS) models along the same lines. Another one is to view the Ising model as a special case ($n = 1$) of the dilute $\mathcal{O}(n)$ loop model.[59] In the loop model case, the $p(\mu_i)$ are the probabilities that the equator of the sphere is run across by loops at positions μ_i. In that case, we would find a universal curve $S_0(n)$ extending Eq. (67).

VI. SCALING OF THE LARGEST PROBABILITY

In this section, we study the scaling of the largest probability

$$p_0 := \max_i p_i = |\langle i_0 | g \rangle|^2, \qquad (72)$$

i.e., the weight of the most probable configuration i_0 in the 1D wave function $|g\rangle$. In terms of a 2D RK state, this corresponds to the largest eigenvalue of the reduced density matrix ρ_A of a half-cylinder. Very similarly to the entropy S, we find that $-\log p_0$ exhibits a linear scaling with L followed by a subleading universal constant

$$-\log p_0 = \tilde{\alpha} L + \gamma + o(1). \qquad (73)$$

Below we evaluate γ in some critical systems.

TABLE I. Correspondence between the Ising chain in a transverse field and related 2D classical models and the results for the constant part of the entropies $S^{(z)}$ and $S^{(x)}$.

Ising chain in a transverse field [Eq. (63)]	Disordered phase $\mu < 1$	$c = \frac{1}{2}$ critical point $\mu = 1$	Ordered phase $\mu > 1$
Constant part of the entropy	$S_0^{(z)} = 0$ $S_0^{(x)} = 0$	$S_0^{(z)} = -0.4387(1)$ $S_0^{(x)} = S_0^{(z)} + \log 2 = 0.2544(1)$	$S_0^{(z)} = -\log 2$ $S_0^{(x)} = +\log 2$
Eight-vertex model [Eq. (66)]	Small-loop phase (low temperature)		Large-loop phase (high temperature)
2D Ising model [Eq. (64)]	Disordered phase (high temperature)		Ordered phase (low temperature)
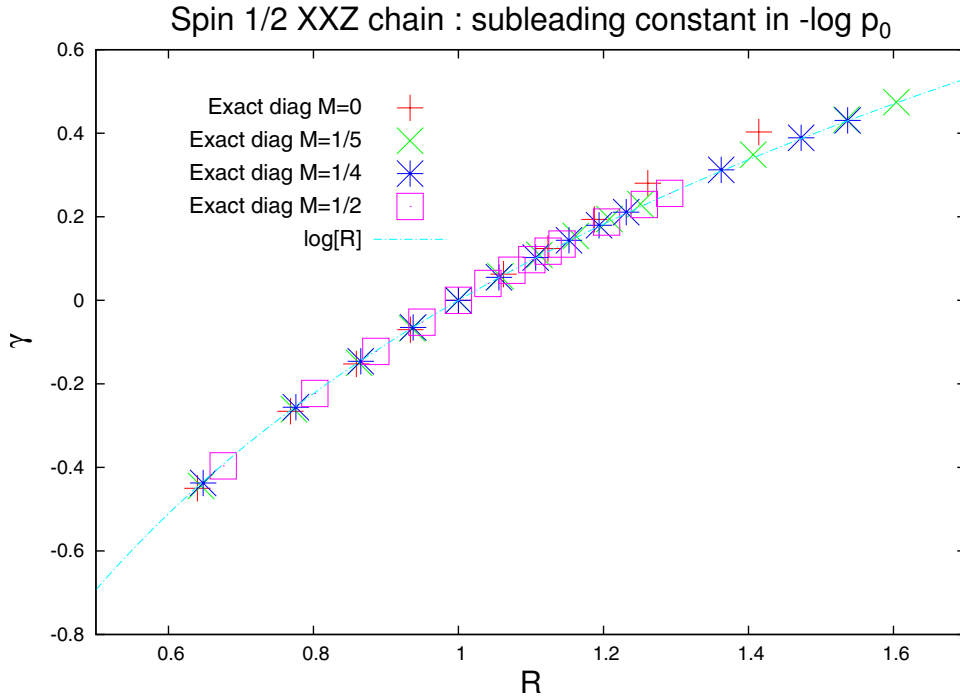
FIG. 13. (Color online) The subleading constant γ in the scaling of $-\log p_0$ [see Eq. (73)] extracted from the critical ground state of the *XXZ* chain in a magnetic field. The same setting as Fig. 8 is taken.

A. $c=1$ critical systems

We first consider the *XXZ* chain in a magnetic field [Eq. (59)] in the critical phase. We find that the largest probability $p_0=|\langle i_0|g\rangle|^2$ is attained by crystal states. For example, $|i_0\rangle = |\uparrow\downarrow\uparrow\downarrow\ldots\rangle$ and $|\downarrow\uparrow\downarrow\uparrow\ldots\rangle$ for $M=0$ and $|i_0\rangle = |\uparrow\uparrow\uparrow\downarrow\uparrow\uparrow\uparrow\downarrow\ldots\rangle$, etc., for $M=1/2$, independent of $\Delta(>-1)$. The constant γ is extracted by fitting finite-size data with Eq. (73). As shown in Fig. 13, we observe a simple relation

$$\gamma = \log R. \tag{74}$$

The same result can be shown exactly for the largest probability $p_0(\beta) := \max p_i(\beta)$ in the Dyson-Gaudin gas when β

$= 2R^2 = 2\lambda$ with $\lambda \in \mathbb{N}$ and $\lambda < \frac{L}{n-1}$ (see Appendix D). For general β, Eq. (74) can be numerically demonstrated as shown in Fig. 14.

In order to understand the connection between S and $-\log p_0$, it is useful to introduce the Rényi entropy,

$$S^{(N)} := \frac{-1}{N-1}\log\left(\sum_i p_i^N\right), \tag{75}$$

where N is a real number. Then, S and $-\log p_0$ correspond to the limits $N \rightarrow 1$ and ∞, respectively. Now we assume that the probability distribution is given by the Boltzmann weights $p_i(\beta) = p_i^{\beta/2}/Z(\beta)$ of the Dyson-Gaudin gas in the critical
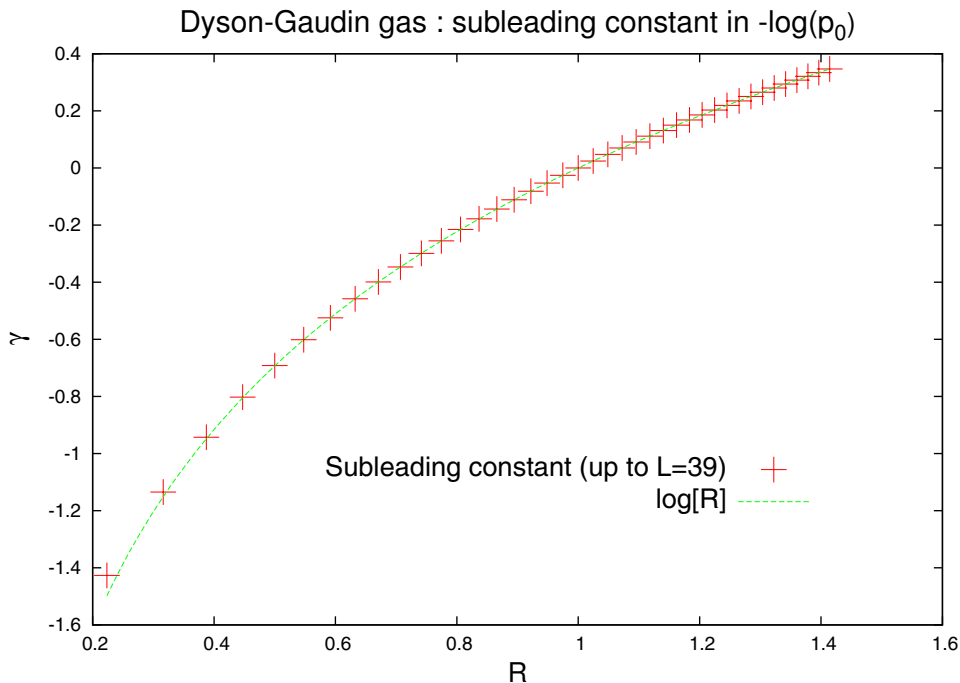
FIG. 14. (Color online) The subleading constant γ in the scaling of $-\log p_0(\beta)$, where $p_0(\beta)$ is the largest probability in the Dyson-Gaudin gas with density $\rho = 1/3$. The data are consistent with Eq. (74). For some special values of R (see the text and Appendix D), Gaudin's formula (33) can be used to show Eq. (74) exactly.
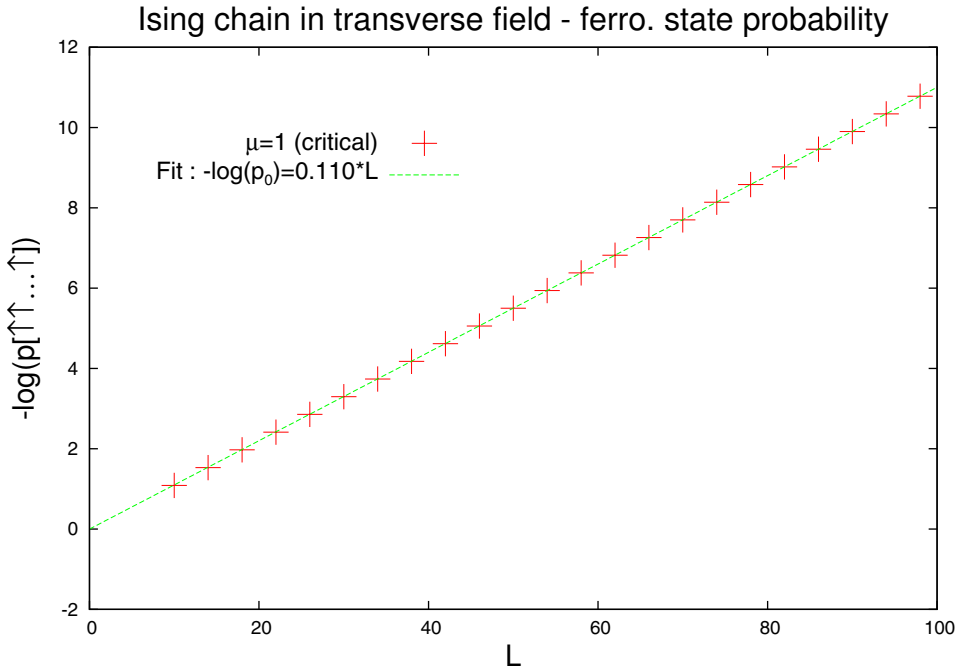
FIG. 15. (Color online) Scaling of $-\log p_0^{(z)}$ in the Ising model in a transverse field at the critical point, calculated in the σ^z basis. The subleading constant $\gamma^{(z)}$ is very close to zero: a fit to the last three points $L=96,98,100$ gives $|\gamma| \le 10^{-6}$.

phase $R=\sqrt{\beta/2}\le d$. The Rényi entropy [Eq. (75)] can then be expressed as

$$S^{(N)}(\beta) = \frac{-1}{N-1}\log\frac{Z(N\beta)}{[Z(\beta)]^N}. \qquad (76)$$

Recalling Eq. (55) for the nonextensive part C of $Z(\beta)$, the subleading constant contribution to $S^{(N)}$ is given by

$$\log R - \frac{1}{2(N-1)}\log N, \quad \sqrt{N}R < R_c = d,$$

$$\frac{N}{N-1}\log R - \frac{1}{N-1}\log d, \quad \sqrt{N}R > R_c = d. \qquad (77)$$

Both expressions give $\gamma = \log R$ in the limit $N\to\infty$. On the other hand, the former expression is consistent with $S_0 = \log R - 1/2$ in the limit $N\to 1$.

An alternative strategy to derive Eq. (74) is to adopt the 2D viewpoint of Sec. II, where the probability p_0 was related to classical partition functions,

$$-\log p_0 = -\log\frac{\mathcal{Z}_{i_0}^A \mathcal{Z}_{i_0}^B}{\mathcal{Z}}. \qquad (78)$$

Here, $\mathcal{Z}_{i_0}^A$ and $\mathcal{Z}_{i_0}^B$ are partition functions on A and B with spins fixed in a state i_0 at their common boundary. Now we move on to the continuum limit described by the action [Eq. (3)]. Recalling that i_0 is given by a crystal state, the above boundary condition corresponds to locking the field ϕ at a certain constant at the boundary (Dirichlet boundary condition).[60] Hence, we obtain

$$-\log p_0 = -\log\frac{\mathcal{Z}_D^A \mathcal{Z}_D^B}{\mathcal{Z}}, \qquad (79)$$

where D stands for Dirichlet. This expression has been evaluated by Hsu *et al.*[24] and by Campos Venuti *et al.*[31] using boundary CFT. Their results for the nonextensive part are consistent with Eq. (74).[61]

In fact, Hsu *et al.*[24] proposed the right-hand side of Eq. (79) as the expression of the entanglement entropy S^{vN} of a half-cylinder. Their argument was based on a replica trick; the Nth moment $\mathcal{M}^{(N)} := \operatorname{Tr} \rho_A^N = \Sigma_i p_i^N$ of the reduced density matrix was evaluated for integer $N\ge 2$ and then an analytic continuation $N\to 1$ was taken. According to their evaluation, the Rényi entropy $S^{(N)} = \frac{-1}{N-1}\log\mathcal{M}^{(N)}$ is expressed by the rhs of Eq. (79) for any integer $N\ge 2$, leading to an *N-independent* subleading constant $\log R$. On the other hand, we have obtained N-*dependent* constant [Eq. (77)]. The two results for the subleading constant agree only in the limit $N\to\infty$. We infer that this discrepancy comes from a difficulty in specifying boundary conditions in the argument of Hsu *et al.*[24] In their argument, they took linear combinations of plural compactified fields, which could make the compactification conditions ambiguous. A more careful treatment of the compactification conditions and a derivation of Eq. (77) in boundary CFT are left as important open issues.

B. $c=1/2$ critical system and beyond

We next consider the Ising chain in a transverse field [Eq. (63)] at the $c=1/2$ critical point $\mu=1$. Figure 15 shows the scaling of $-\log p_0^{(z)}$ in the σ^z basis. Here, the largest probability is attained by the ferromagnetic configuration $|i_0\rangle = |\uparrow\uparrow\uparrow\ldots\rangle_z$. In this case we have the following exact formula (see Appendix E 3):

$$p_0^{(z)} = \prod_{j=1}^{L/2} \cos^2\left(\frac{(2j-1)\pi}{4L}\right). \tag{80}$$

An Euler-Maclaurin expansion shows that the subleading constant is $\gamma^{(z)} = 0$. The data in Figure 15 are consistent with this result and give $\gamma^{(z)} < 10^{-6}$. It can also be shown that $\gamma^{(z)}$ remains zero away from the critical point. Moving to the σ^x basis using the same argument leading to Eq. (71), we obtain $\gamma^{(x)} = \log 2$.

In a 2D viewpoint, p_0 is related to a ratio of partition functions, as shown in Eq. (78). Since the boundary configurations, a_h and b_h, at the upper and lower edges of the cylinder were arbitrary, we can glue these edges by identifying a_h and b_h and integrating them out. Algebraically, we consider

$$p_0 = \frac{\langle i_0 | \mathcal{T}^{2h} | i_0 \rangle}{\mathrm{Tr}\, \mathcal{T}^{2h}} = \frac{\mathcal{Z}_{i_0 i_0}(L, 2h)}{\mathcal{Z}_P(L, 2h)} \quad (h \to \infty). \tag{81}$$

Here, the numerator $\mathcal{Z}_{i_0 i_0}$ is the partition function of a long cylinder with boundary configurations fixed in the same state i_0 at both edges. The denominator $\mathcal{Z}_P$ is the partition function of a torus.

A similar quantity has been considered in a rational CFT context. Therein, the fixed boundary conditions imposed in the numerator of Eq. (81) are replaced by conformally invariant ones a. The associated probability p_a can be evaluated as explained in Ref. 62. In the notations in Ref. 62, the result is

$$p_a = \frac{(\psi_a^1)^2}{S_1^1}, \tag{82}$$

where ψ_a^j are certain structure constants, characteristic of the model, and S_1^1 is the identity matrix element of the S matrix implementing the modular transformation. In the simplest case of an A_m $SU(2)_k$ model, the boundary fields correspond to the vertices of the A_m Dynkin diagram. Let $\{d_a\}$ be the Perron-Frobenius eigenvector of the A_m incidence matrix, normalized so that $d_1 = 1$. Then, each d_a is the so-called quantum dimension of the state a, and $d = \sqrt{\sum_a d_a^2}$ is called the total quantum dimension. In this case, $\psi_a = d_a/d$ and $S_1 = 1/d$, hence

$$p_a = \frac{d_a^2}{d}. \tag{83}$$

We study the case where the Dynkin diagram is A_3 and the possible states are +, free, − with quantum dimensions 1, $\sqrt{2}$, 1, respectively. The probabilities are, in the σ^x basis,

$$p_+ = p_- = \frac{1}{2}, \quad p_{\mathrm{free}} = 1. \tag{84}$$

A_3 also describes the Ising model and this enables us to confirm the numerical results at the beginning of this section. The ferromagnetic state in the σ^z basis, $|\uparrow\uparrow\uparrow\ldots\uparrow\rangle_z$, may be regarded as a paramagnetic state in the σ^x basis or the "free" state in CFT. Equation (84) then gives

$$\gamma^{(z)} = -\log p_{\mathrm{free}} = 0, \tag{85}$$

in agreement with our numerical result. The largest probability p_0 in the σ^x basis may be regarded as the probability of the "+" state in CFT, hence

$$\gamma^{(x)} = -\log p_+ = \log 2, \tag{86}$$

in agreement with our calculation.

These results can be extended to A_m RSOS models with central charge $c < 1$. p_0 is in this case with highest probability is in this case

$$p_0 = 2\sqrt{\frac{2}{m(m+1)}} \sin\left(\frac{\pi}{m+1}\right) \sin\left(\frac{\pi}{m}\right). \tag{87}$$

VII. SUMMARY AND CONCLUSIONS

The starting point of this study was to introduce the Shannon entropy of a 1D ground-state wave function, which measures quantum fluctuations occurring in a given basis.

Like other entanglement measures, we have seen that the scaling behavior of this entropy is essentially controlled by the long-distance correlations. Using a transfer matrix approach, we showed that this entropy can also be interpreted as the entanglement entropy of a half-cylinder for a suitably chosen 2D RK state. This correspondence allowed us to study the entanglement entropy of 2D wave functions using simpler 1D systems, without the need to trace explicitly over the degrees of freedom sitting outside of the subsystem (a formidable task in two dimensions).

To unveil the generic scaling properties of the Shannon entropy of 1D states (equal to the entanglement entropy of 2D states), we have studied several 1D quantum systems: (i) a discretized version of the Dyson gas/Calogero-Sutherland ground-state wave function (relevant to 2D dimer RK states) in Sec. III, (ii) the spin-$\frac{1}{2}$ XXZ chain (relevant to six-vertex RK states) in Sec. IV, and (iii) the Ising chain in transverse field (relevant to 2D Ising RK states and 2D eight-vertex RK states) in Sec. V.

In both critical and massive systems, we found that this entropy is composed of an extensive part and a subleading constant S_0. There is no logarithmic contribution as anticipated before for half-cylinder geometry.[23,24] For Tomonaga-Luttinger liquids [cases (i) and (ii) above], described by a compactified boson with radius R, we showed numerically and analytically that $S_0 = \log R - \frac{1}{2}$ (a result which *differs* from the recent prediction by Hsu *et al.*[24]). Going back to the 2D entanglement entropy interpretation of this result, it implies that the usual RK states for dimers on the hexagonal or square lattice (with $R = 1$) have $S_0 = -\frac{1}{2}$. At present, we do not have a derivation for the value $S_0^{(z)} = -0.4387$ (or $S_0^{(x)} = -0.4387 + \log 2$ depending on the choice of the basis) found numerically for the Ising chain in transverse field at its $c = 1/2$ critical point.

We introduced a temperature β^{-1} to extend the Shannon and entanglement entropies in Sec. II D. This has different consequences depending on the nature of the criticality. For TLLs, changing β gives a natural way to tune the boson
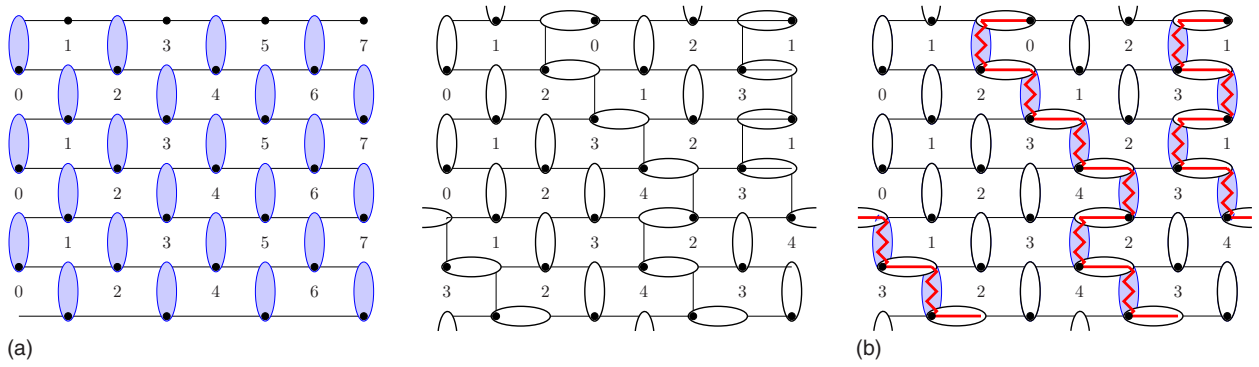
FIG. 16. (Color online) (a) left: reference configuration. (a) right: real configuration. (b): transition graph. Reference dimers are in blue. The fermions are living on the vertical edges of the lattice and are symbolized by red zigzag lines. The integers attached to each plaquette of the lattice form a height configuration associated to the dimer covering. When coarse grained, these microscopic heights become the free field which describe the long-distance properties of the system (Refs. 63 and 64). The heights can be constructed by fixing $h=0$ at some origin and then moving from plaquette to plaquette by turning clockwise around the sites of the even sublattice (marked with a black dot). The rule is the following: the height picks a contribution equal to $+2$ when crossing a dimer and -1 otherwise. Since there is exactly one dimer touching each site, the height difference between two points does not depend on the chosen path on a simply connected domain. With periodic boundary conditions, the height is not single valued. For example, when winding horizontally around the system, the height picks a contribution W_x (also called winding number) equal to twice the number of vertical dimers crossed minus the number of empty bonds. Inserting a fermionic world line going upward shifts the height by -3 by going from the left to the right and thus changes $W_x \to W_x - 3$. It is simple to check that the configurations with a fermion density equal to $\frac{2}{3}$ have $W_x = 0$ and an average "slope" equal to zero.

radius R while retaining the $c=1$ criticality. This allowed us to "deform" a dimer RK problem (or a free fermion problem) and to derive the R dependence of the entropy constant S_0 in Sec. III. When β reaches a critical value, the system undergoes a phase transition to a crystal state, where the entropy constant takes a stable value $S_0 = \log d$, with d being the degeneracy of the ground states. Hence, this transition can be detected through S_0. In contrast, in the critical Ising chain with $c=1/2$, the entropy constant S_0 shows an abrupt change around $\beta=2$. More generally, the β dependence might offer a valuable fingerprint for clarifying the nature of the undeformed case $\beta=2$.

We also considered the scaling properties of p_0, the probability of the most likely configuration in a critical 1D state (Sec. VI). This quantity, which corresponds to the largest eigenvalue of the reduced density matrix in the 2D point of view, also contains a universal constant contribution γ in critical states. We found numerically and analytically that $\gamma = \log R$ for TLL states and $\gamma^{(z)}=0$ and $\gamma^{(x)}=\log 2$ for the critical Ising chain. These are related to the probabilities associated with conformally invariant boundary conditions.

The universal R dependence of S_0 and γ found in the present work can be used as a new simple way to determine the boson radius R in a TLL through a ground-state structure. Similar universal R dependence was also found in the mutual information (double-interval entanglement entropy) studied in Refs. 7 and 8. Notice that the mutual information is invariant under the transformation $R \to 2/R$ while the present quantities are not. This difference is related to the origins of the R dependence: it comes from certain boundary effects in the present case, while it comes from the special topologies of the Riemann surfaces in the case of the mutual information.[7,8]

In fact, the transfer matrix approach gives access to *all* the eigenvalues $\{p_i\}$ of reduced density matrix ρ_A of a half-

cylinder. (As a first application, the gap p_1/p_0 is computed in Appendix D for dimers on the hexagonal lattice). The present approach therefore provides a convenient tool to study the properties of the "entanglement spectrum"[39] in a 2D quantum state.

ACKNOWLEDGMENTS

APPENDIX A: FREE FERMIONS AND WICK'S THEOREM

The probabilities of Eq. (26) involve quantities such as $\langle 0|a_1 a_2 \ldots a_{2n}|0\rangle$, where the a_j are linear combinations of fermion creation and annihilation operators. Wick's theorem then gives

$$\langle 0|a_1 \ldots a_{2n}|0\rangle = \langle a_1 \ldots a_{2n}\rangle = \sum_{\substack{i_1 < \ldots < i_n \\ \forall\ k, i_k < j_k}} \epsilon(\sigma)$$
$$\times \langle a_{i_1} a_{j_1}\rangle \ldots \langle a_{i_n} a_{j_n}\rangle = \text{Pf}\, A, \quad \text{(A1)}$$

where $\epsilon(\sigma)$ is the signature of the permutation which transforms $\{1, 2, \ldots, 2n\}$ into $\{i_1, j_1, i_2, j_2, \ldots, i_n, j_n\}$. Pf denotes the Pfaffian. A is an antisymmetric $2n \times 2n$ matrix given by

$$A = \begin{bmatrix} 0 & \langle a_1 a_2\rangle & \ldots & \langle a_1 a_{2n}\rangle \\ -\langle a_1 a_2\rangle & 0 & \ldots & \langle a_2 a_{2n}\rangle \\ \vdots & \vdots & \ddots & \vdots \\ -\langle a_1 a_{2n}\rangle & -\langle a_2 a_{2n}\rangle & \ldots & 0 \end{bmatrix}. \quad \text{(A2)}$$

The two following properties of Pfaffians are useful,

$$(\text{Pf } A)^2 = \det A, \tag{A3}$$

$$\text{Pf}\begin{bmatrix} 0 & B \\ -B^T & 0 \end{bmatrix} = \pm \det B, \tag{A4}$$

and allow fast numerical calculations using determinant routines.

APPENDIX B: TRANSFER MATRIX FOR THE CLASSICAL DIMER MODEL ON THE HEXAGONAL LATTICE

1. Transfer matrix as free fermions

Here we consider a hexagonal lattice with periodic boundary conditions and an even number of columns L. The mapping onto free fermions is as follows (see Fig. 16):

We choose a convenient dimer configuration which we call a reference configuration. Any other dimer configuration (real configuration) will be compared to the reference by superposition of the two. We define the particle locations as the vertical edges that are not occupied by a "real" dimer (only a reference one). Particles can jump from a vertical edge to another only if a real horizontal dimer connects the two. This mapping has several interesting properties:

(i) The dimer configuration is totally determined by the trajectories of the particles.

(ii) Two particles cannot go to the same edge. Therefore, they obey a fermionic exclusion rule. This encodes the dimer hardcore constraint.

(iii) The number of fermions is conserved, so that the TM is block diagonal, each block corresponding to a fixed number of fermions. It should be remarked that this property would not hold on nonbipartite lattices (such as the triangular).

2. Fermionic representation and periodic boundary conditions

A state of a row is determined by the number n of fermions and their positions $0 \leq \alpha_1 < \ldots < \alpha_n \leq L-1$. We can choose to represent such a state using second-quantized fermion creation operators,

$$|i\rangle = |\alpha_1 \ldots \alpha_n\rangle = c_{\alpha_1}^\dagger \ldots c_{\alpha_n}^\dagger |0\rangle. \tag{B1}$$

As we want to use the translational invariance, we have to set

$$|\alpha_1, \ldots, \alpha_{n-1}, L\rangle = |0, \alpha_1, \ldots, \alpha_{n-1}\rangle. \tag{B2}$$

Therefore, to keep the order of Eq. (B1),

$$c_L^\dagger = (-1)^{\hat{n}-1} c_0^\dagger, \quad \hat{n} = \sum_{j=0}^{L-1} c_j^\dagger c_j. \tag{B3}$$

In the following, we will also need the L fermion operators in Fourier space,

$$c_k^\dagger = \frac{1}{\sqrt{L}} \sum_{j=0}^{L-1} e^{-ikj} c_j^\dagger. \tag{B4}$$

They satisfy $\{c_k, c_{k'}^\dagger\} = \delta_{kk'}$, provided $e^{ikL} = (-1)^{\hat{n}-1}$. The set of wave vectors is given by
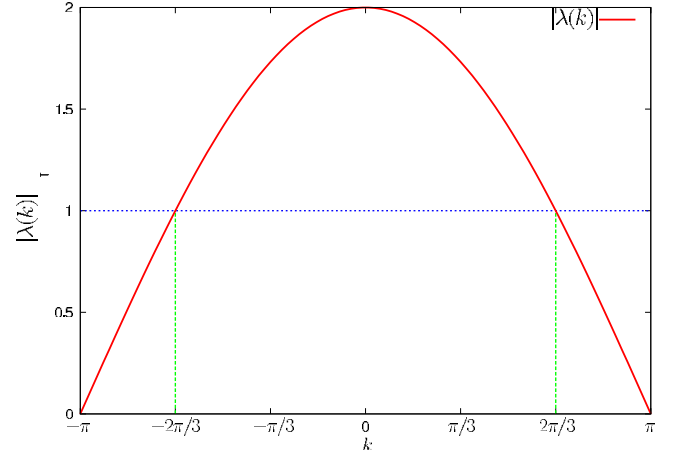
FIG. 17. (Color online) One-particle eigenvalue as a function of k.

$$k \in \left\{ -\pi + \frac{\pi}{L} + \frac{2\pi l}{L} \,\middle|\, l = 0, \ldots, L-1 \right\}, \quad \hat{n} \text{ even,}$$

$$k \in \left\{ -\pi + \frac{2\pi l}{L} \,\middle|\, l = 0, \ldots, L-1 \right\}, \quad \hat{n} \text{ odd.}$$

3. Diagonalization of the transfer matrix

Each fermion can go to the left or to the right with equal amplitude. We number vertical edges in such a way that a fermion located on j can go to j or $j+1$. $\mathcal{T}$ satisfies

$$\mathcal{T}|0\rangle = |0\rangle, \tag{B5}$$

$$\mathcal{T} c_j^\dagger \mathcal{T}^{-1} = c_j^\dagger + c_{j+1}^\dagger. \tag{B6}$$

So that

$$\mathcal{T} c_k^\dagger \mathcal{T}^{-1} = \lambda(k) c_k^\dagger, \quad \lambda(k) = 1 + e^{ik}, \tag{B7}$$

$c_k^\dagger |0\rangle$ is then eigenvector of $\mathcal{T}$ with eigenvalue $\lambda(k)$. In a similar manner,

$$\mathcal{T} c_{k_1}^\dagger c_{k_2}^\dagger \ldots c_{k_n}^\dagger \mathcal{T}^{-1} = \lambda(k_1) \ldots \lambda(k_n) c_{k_1}^\dagger \ldots c_{k_n}^\dagger. \tag{B8}$$

Provided all the wave vectors are different, $c_{k_1}^\dagger \ldots c_{k_n}^\dagger |0\rangle$ is an eigenvector with eigenvalue $\lambda(k_1) \ldots \lambda(k_n)$. The transfer matrix can also be expressed explicitly,

$$\mathcal{T} = \prod_k (1 + e^{ik} c_k^\dagger c_k). \tag{B9}$$

4. Largest eigenvalue and dominant eigenvector

Since $|\lambda(k)| \geq 1$ for every $k \in [-2\pi/3, 2\pi/3]$ (see Fig. 17), the eigenvalue with largest modulus in a given sector with n fermions is obtained by a product over the n nearest to 0 wave vectors. Let us denote this eigenvalue by Λ_n. Then, $\Lambda_{\max} = \max\{|\Lambda_n|, 1 \leq n \leq L\}$. The eigenvalue with largest modulus is real and has approximately all allowed k lying in the interval $[-2\pi/3, 2\pi/3]$. The dominant sector has there-
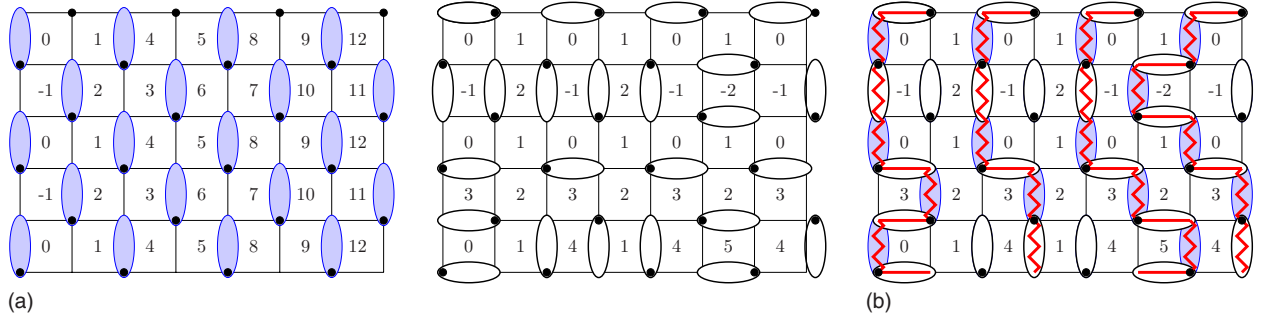
FIG. 18. (Color online) Upper left: reference configuration. Upper right: chosen configuration. Below: the fermions are living on the vertical edges of the lattice and are symbolized by red zigzag lines. Edges are numbered from 0 to $L-1$. The integers attached to each plaquette form a height configuration associated to the dimer covering. The rule is very similar to that of the honeycomb lattice: turning clockwise around the sites of the even sublattice (marked with black dots), the height picks a contribution equal to $+3$ when crossing a dimer and -1 otherwise. $h=0$ is fixed at some origin. For a more detailed presentation, see Ref. 65.

fore $n \simeq 2L/3$ fermions. It is easy to understand the fact that the "dominant" fermion density is $2/3$: it corresponds to flat height configurations (see Fig. 16).

If we denote by Ω the set of wave vectors that gives the largest eigenvalue then the dominant eigenvector is

$$|g\rangle = \left(\prod_{k \in \Omega} c_k^\dagger \right) |0\rangle. \qquad (B10)$$

Let us show what is Ω in the simple case where $L=6p$. We have to distinguish between the even and odd sectors,

$$\Lambda_{\max}^{(e)} = \max\{\Lambda_{2n'}\} = \prod_{l=p}^{5p-1} \lambda\left(-\pi + \pi \frac{2l+1}{6p} \right),$$

$$\Lambda_{\max}^{(o)} = \max\{\Lambda_{2n'+1}\} = \prod_{l=p}^{5p} \lambda\left(-\pi + \frac{\pi l}{3p} \right). \qquad (B11)$$

Here, $\Lambda_{\max}^{(e)} > \Lambda_{\max}^{(o)}$ because Euler-Maclaurin expansion gives $\log \Lambda_{\max}^{(e)} - \log \Lambda_{\max}^{(o)} = \frac{\pi\sqrt{3}}{24p} + o(1/p)$. Therefore the leading eigenvalue corresponds to $4p = \frac{2}{3}L$ fermions and

$$\Omega = \left\{ -\pi + \pi \frac{2l+1}{6p} \,\middle|\, p \leq l \leq 5p-1 \right\}. \qquad (B12)$$

5. Probability of a given configuration

The dominant eigenvector has $n = 2L/3$ fermions. A configuration i is represented by

$$|i\rangle = c_{\alpha_1}^\dagger \dots c_{\alpha_n}^\dagger |0\rangle \qquad (B13)$$

and will have a probability [we use Eqs. (A1) and (A4)]

$$p_i = |\langle 0|c_{\alpha_n} \dots c_{\alpha_1} c_{k_1}^\dagger \dots c_{k_n}^\dagger |0\rangle|^2 \qquad (B14)$$

$$= \left(\frac{1}{L}\right)^n |\det(e^{-i\alpha_j k_{j'}})_{jj'}|^2. \qquad (B15)$$

We get a Vandermonde determinant and p_i simplifies into Eq. (30).

APPENDIX C: TRANSFER MATRIX FOR THE CLASSICAL DIMER MODEL ON THE SQUARE LATTICE

1. Free fermions

We consider a square lattice with periodic boundary conditions and an even number of columns L. The mapping is similar to that of the hexagonal lattice. The reference configuration is shown in Fig. 18. Here, a fermion will be defined as an even vertical edge occupied only by a reference dimer or an odd vertical edge occupied only by a real dimer. It can go to the left, straight ahead, or to the right. We introduce a shift in the numbering, so that a fermion located on site j can go to j, $j+1$, or $j+2$.

2. Diagonalization of the transfer matrix

As for the honeycomb case, $\mathcal{T}$ is block diagonal and invariant by translation. It also satisfies

$$\mathcal{T}|0\rangle = |0\rangle, \qquad (C1)$$

$$\mathcal{T}c_{2j}^\dagger \mathcal{T}^{-1} = c_{2j+2}^\dagger + c_{2j+1}^\dagger + c_{2j}^\dagger, \qquad (C2)$$

$$\mathcal{T}c_{2j+1}^\dagger \mathcal{T}^{-1} = c_{2j+2}^\dagger. \qquad (C3)$$

As usual we also define Fourier-space fermions,

$$c_{0k}^\dagger = \frac{1}{\sqrt{L/2}} \sum_j e^{-ik2j} c_{2j}^\dagger, \qquad (C4)$$

$$c_{1k}^\dagger = \frac{1}{\sqrt{L/2}} \sum_j e^{-ik(2j+1)} c_{2j+1}^\dagger, \qquad (C5)$$

with

$$k \in \left\{ -\frac{\pi}{2} + \frac{\pi}{L} + \frac{2\pi l}{L} \,\middle|\, l = 0, \dots, \frac{L}{2} - 1 \right\}, \quad \hat{n} \text{ even},$$

$$k \in \left\{ -\frac{\pi}{2} + \frac{2\pi l}{L} \,\middle|\, l = 0, \dots, \frac{L}{2} - 1 \right\}, \quad \hat{n} \text{ odd}.$$

The transfer matrix acts on them in the following way:
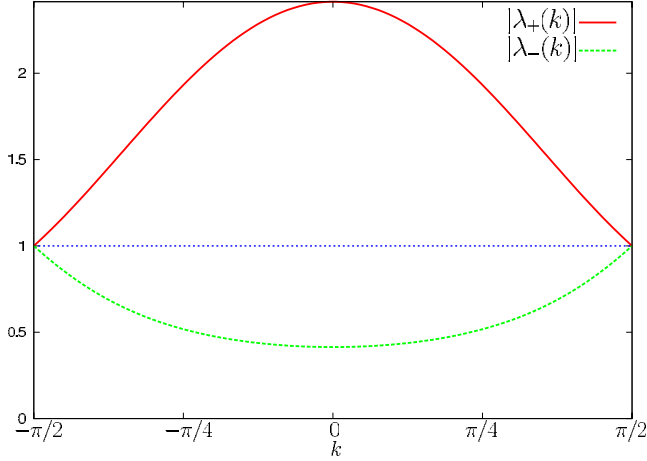
FIG. 19. (Color online) One-particle eigenvalues λ_+ and λ_- as a function of k.

$$\mathcal{T}c_{0k}^{\dagger}\mathcal{T}^{-1} = (1 + e^{2ik})c_{0k}^{\dagger} + e^{ik}c_{1k}^{\dagger}, \quad (C6)$$

$$\mathcal{T}c_{1k}^{\dagger}\mathcal{T}^{-1} = e^{ik}c_{0k}^{\dagger}. \quad (C7)$$

To diagonalize $\mathcal{T}$, it is therefore sufficient to diagonalize a 2×2 matrix,

$$M = \begin{pmatrix} 1 + e^{2ik} & e^{ik} \\ e^{ik} & 0 \end{pmatrix}. \quad (C8)$$

If one sets

$$\tan \theta_k = \sqrt{1 + \cos^2 k} - \cos k, \quad (C9)$$

$$\lambda_{\pm}(k) = e^{ik}(\cos k \pm \sqrt{1 + \cos^2 k}), \quad (C10)$$

$$b_{+k}^{\dagger} = \cos \theta_k c_{0k}^{\dagger} + \sin \theta_k c_{1k}^{\dagger}, \quad (C11)$$

$$b_{-k}^{\dagger} = -\sin \theta_k c_{0k}^{\dagger} + \cos \theta_k c_{1k}^{\dagger}, \quad (C12)$$

then

$$\mathcal{T}b_{+k}^{\dagger}\mathcal{T}^{-1} = \lambda_+(k)b_{+k}^{\dagger}, \quad (C13)$$

$$\mathcal{T}b_{-k}^{\dagger}\mathcal{T}^{-1} = \lambda_-(k)b_{-k}^{\dagger}, \quad (C14)$$

which gives us all the eigenvalues and eigenvectors of $\mathcal{T}$. It is also possible to express explicitly $\mathcal{T}$,

$$\mathcal{T} = \prod_k \{1 + [\lambda_+(k) - 1]b_{+k}^{\dagger}b_{+k}\}\{1 + [\lambda_-(k) - 1]b_{-k}^{\dagger}b_{-k}\}.$$

3. Largest eigenvalue and dominant eigenvector

We assume for simplicity that L is a multiple of 4. Noticing (see Fig. 19) that $\forall \; k, |\lambda_+(k)| \geq 1$ and also $|\lambda_-(k)| \leq 1$, we can deduce that only the $\lambda_+(k)$ will contribute to the largest eigenvalue. In Ref. 65 it is shown that

$$\lambda_{\max} = \prod_{k \in \Omega} \lambda_+(k), \quad (C15)$$

where $\Omega = \{-\frac{\pi}{2} + \frac{\pi}{L} + \frac{2\pi}{L}l \,|\, l = 0 \cdots L/2 - 1\}$. The leading sector has an even number of fermions $L/2$ and the dominant eigenvector will be given by

$$|g\rangle = \left(\prod_{k \in \Omega} b_{+,k}^{\dagger}\right)|0\rangle. \quad (C16)$$

4. Probability of a given configuration

The dominant eigenvector has $n = L/2$ fermions. A configuration i is represented by

$$|i\rangle = c_{\alpha_1}^{\dagger} \ldots c_{\alpha_n}^{\dagger}|0\rangle \quad (C17)$$

and will have a probability [using Eq. (A1) and also Eq. (A4)]

$$p_i = |\langle 0|c_{\alpha_n} \ldots c_{\alpha_1} b_{+,k_1}^{\dagger} \ldots b_{+,k_n}^{\dagger}|0\rangle|^2 \quad (C18)$$

$$= \left(\frac{2}{L}\right)^n |\det m_{jj'}|^2, \quad (C19)$$

where

$$m_{jj'} = \begin{cases} \cos \theta_{k_j} e^{i\alpha_j k_{j'}}, & \alpha_j \text{ even} \\ \sin \theta_{k_j} e^{i\alpha_j k_{j'}}, & \alpha_j \text{ odd}. \end{cases} \quad (C20)$$

This determinant is slightly more complicated than on the honeycomb lattice and cannot be further simplified.

APPENDIX D: 2D COULOMB GAS ON A CIRCLE

We consider a Gaudin model with n charges dispatched on a circle with L sites.

1. Scaling of the ground state

We study the special case where $L/n \in \mathbb{N}$ and we set $\rho = n/L$. We denote by $p_0(\beta)$ the probability associated with the ground-state configuration. It corresponds to the case where the distance between each charges is maximal. Therefore it is obtained when all charges lie on the edges of a polygon. Hence,

$$p_0(\beta) = \frac{1}{Z_n^{(L)}(\beta)} L^{-n\beta/2} \prod_{1 \leq k < l \leq n} |e^{2il\pi/n} - e^{2ik\pi/n}|^{\beta}.$$

Using the formula $\prod_{l=1}^{n-1}(1 - e^{2il\pi/n}) = n$, we get

$$p_0(\beta) = \frac{\rho^{n\beta/2}}{Z_n^{(N)}(\beta)}. \quad (D1)$$

In the special case where β is an even integer and $\beta < \frac{2L}{n-1}$, it is possible to use Eq. (33) and the subleading term of $-\log p_0(\beta)$ can easily be found,

$$-\log p_0(\beta) = an + \frac{1}{2}\log\frac{\beta}{2}. \quad (D2)$$

This result for the universal part of the probability, $\gamma = \frac{1}{2}\log\frac{\beta}{2} = \log R$, does not depend on L nor n (no finite-size effects).

2. Existence of a gap in the thermodynamical limit

The first excitation is obtained from the ground-state configuration by moving one particle to the next site while keeping all the others in place. The associated probability $p_1(\beta)$ will be given by

$$\frac{p_1(\beta)}{p_0(\beta)} = \left[\prod_{l=1}^{n-1} \frac{\sin\left(\dfrac{l\pi}{n} - \dfrac{\rho l\pi}{n}\right)}{\sin\left(\dfrac{l\pi}{n}\right)} \right]^{\beta}. \tag{D3}$$

In the limit $n \to +\infty$ it is possible to expand the sin,

$$\frac{p_1(\beta)}{p_0(\beta)} = \left[\prod_{l=1}^{n-1} \left(1 - \frac{\rho\pi}{n}\cot(l\pi/n) \right) \right]^{\beta}. \tag{D4}$$

We then consider $P_n(x) = \prod_{l=1}^{n-1}[1 - x\cot(l\pi/n)]$. The trick to calculate $P_n(x)$ is to introduce another polynomial $Q_n(x)$ which satisfies

$$Q_n(\tan t) = \frac{\sin nt}{(\sin t)\cos^{n-1} t}. \tag{D5}$$

$Q_n(x)$ and $P_n(x)$ are of the same degree and share the same zeros: they have to be proportional. $P_n(0)=1$ and $Q_n(0)=n$ yield $P_n(x) = \frac{1}{n}Q_n(x)$. Using Eq. (D5) and Moivre's formula, we get

$$P_n(x) = \frac{1}{n} \sum_{k=0}^{[(n-1)/2]} (-1)^k C_n^{2k+1} x^{2k}. \tag{D6}$$

Therefore $P_n(\frac{\pi\rho}{n})$ reduces in the limit $n \to \infty$ to

$$P_n\left(\frac{\pi\rho}{n}\right) = \frac{1}{\pi\rho}\sin(\pi\rho). \tag{D7}$$

Finally,

$$\frac{p_1(\beta)}{p_0(\beta)} = \left[\frac{1}{\pi\rho}\sin(\pi\rho) \right]^{\beta}. \tag{D8}$$

So that there is a finite gap in the thermodynamical limit,

$$\Delta E = E_1 - E_0 = -\log\left[\frac{1}{\pi\rho}\sin(\pi\rho) \right]. \tag{D9}$$

This calculation can easily be extended (in the thermodynamical limit) to any configuration deduced from the ground state by moving a finite number of particle. For the corresponding RK wave function, ΔE gives an information about the first gap of the reduced density matrix (entanglement spectrum).

APPENDIX E: GROUND STATE OF THE ISING CHAIN IN A TRANSVERSE FIELD

1. Diagonalization

We consider the Hamiltonian of an Ising chain in a transverse field with an *even* number of sites L,

$$\mathcal{H} = -\mu\sum_{j=0}^{L-1} \sigma_j^x \sigma_{j+1}^x - \sum_{j=0}^{L-1} \sigma_j^z. \tag{E1}$$

Using a Jordan-Wigner transformation,

$$\sigma_j^+ = \frac{\sigma_j^x + i\sigma_j^y}{2} = c_j^\dagger \exp\left(i\pi\sum_{l=0}^{j-1} c_l^\dagger c_l \right), \tag{E2}$$

$$\sigma_j^z = 2c_j^\dagger c_j - 1, \tag{E3}$$

$\mathcal{H}$ is rewritten as

$$\mathcal{H} = -\sum_{j=0}^{L-1} (2c_j^\dagger c_j - 1) - \mu\sum_{j=0}^{L-2} (c_j^\dagger - c_j)(c_{j+1}^\dagger + c_{j+1}) + \mu(c_{L-1}^\dagger - c_{L-1})(c_0^\dagger + c_0)e^{i\pi\mathcal{N}}, \tag{E4}$$

where $\mathcal{N} = \sum_{j=0}^{L-1} c_j^\dagger c_j$ is the fermion number operator. Since $\mathcal{P} = \prod_{j=0}^{L-1} \sigma_j^z = \pm 1$ is a conserved quantity, $\mathcal{H}$ may be separately diagonalized in two sectors. Here we are only interested in the ground state of the chain. In the basis of the eigenstates of the σ_j^z, all off-diagonal elements are negative, and it lies in the sector $\mathcal{P} = +1$ (Perron-Frobenius theorem). Using $\mathcal{P} = \exp(i\pi\mathcal{N})$ and the last term of Eq. (E4), we see that in this sector, one has to keep configurations with an even number of fermions satisfying antiperiodic boundary conditions

$$c_L^\dagger = -c_0^\dagger. \tag{E5}$$

To take advantage of the translational invariance, we introduce Fourier-space fermions

$$c_k^\dagger = \frac{1}{\sqrt{L}}\sum_{j=0}^{L-1} e^{-ikj}c_j^\dagger, \tag{E6}$$

where $k \in \{(2l+1)\frac{\pi}{L} \,|\, -L/2 \le l \le L/2-1\}$ are the L wave vectors. The Hamiltonian becomes

$$\mathcal{H} = L - \sum_k 2(1 + \mu\cos k)c_k^\dagger c_k + \mu\sum_k (i\sin k c_k^\dagger c_{-k}^\dagger - i\sin k c_{-k}c_k). \tag{E7}$$

This expression can be diagonalized using a Bogoliubov transformation,

$$c_k^\dagger = \cos\theta_k b_k - i\sin\theta_k b_{-k}^\dagger, \tag{E8}$$

$$\theta_{-k} = -\theta_k, \tag{E9}$$

provided the following condition is satisfied:

$$\tan 2\theta_k = \frac{\mu\sin k}{1 + \mu\cos k}. \tag{E10}$$

We then obtain

$$\mathcal{H} = \sum_k \varepsilon(k)[b_k^\dagger b_k - 1/2], \tag{E11}$$

$$\frac{\varepsilon(k)}{2} = (1 + \mu \cos k)\cos 2\theta_k + \mu \sin k \sin 2\theta_k. \quad \text{(E12)}$$

In the following, we want the vacuum of the b_k to be the ground state of $\mathcal{H}$, which is true only if $\varepsilon(k) > 0 \ \forall \ k$. One also has to take into account the indetermination of $\theta \mod \pi$. There are two cases.

(i) $\mu \leq 1$: Here $1 + \mu \cos k$ is always positive. We choose

$$\theta_k = \frac{1}{2}\arctan\left(\frac{\mu \sin k}{1 + \mu \cos k}\right) \quad \text{(E13)}$$

and the energy spectrum is given by

$$\varepsilon(k) = 2\sqrt{1 + 2\mu \cos k + \mu^2}. \quad \text{(E14)}$$

(ii) $\mu > 1$: Here, one has to be careful because $1 + \mu \cos k$ can vanish and change sign. A generic solution of Eq. (E10) is

$$\theta_k = \frac{1}{2}\arctan\left(\frac{\mu \sin k}{1 + \mu \cos k}\right) + \frac{\pi}{2}q_k, \quad q_k \in \mathbb{Z}. \quad \text{(E15)}$$

The eigenenergies are given by

$$\varepsilon(k) = (-1)^{q_k}\,\mathrm{sgn}(1 + \mu \cos k)2\sqrt{1 + 2\mu \cos k + \mu^2}. \quad \text{(E16)}$$

$1 + \mu \cos k$ changes sign at $k = \pm k_c = \pm \arccos(-1/\mu)$. A possible choice is therefore

$$q_k = \begin{cases} -1, & k < -k_c \\ 0, & -k_c \leq k \leq k_c \\ 1, & k > k_c. \end{cases} \quad \text{(E17)}$$

2. Probability of a given configuration

Since $|0\rangle$ is the ground state of the chain, the probability of each configuration i is (in the σ^z basis)

$$p_i = \langle 0|P_1^{\uparrow/\downarrow}P_2^{\uparrow/\downarrow}\dots P_L^{\uparrow/\downarrow}|0\rangle, \quad \text{(E18)}$$

where $P_j^{\uparrow}$ ($P_j^{\downarrow}$) is the projector onto the $|\uparrow\rangle_j^z$ ($|\downarrow\rangle_j^z$) state,

$$P_j^{\uparrow} = c_j^{\dagger}c_j, \quad P_j^{\downarrow} = c_j c_j^{\dagger}. \quad \text{(E19)}$$

Using Wick's theorem, p_i reduces to a Pfaffian. To compute it, we need to calculate four types of contractions: $\langle c_j^{\dagger}c_{j'}\rangle$, $\langle c_j c_{j'}^{\dagger}\rangle$, $\langle c_j^{\dagger}c_{j'}^{\dagger}\rangle$, and $\langle c_j c_{j'}\rangle$. This can be done by expressing back the Jordan-Wigner fermions in terms of the Bogoliubov fermions,

$$\langle c_j^{\dagger}c_{j'}\rangle = \frac{1}{L}\sum_k \cos^2 \theta_k \cos[k(j - j')], \quad \text{(E20)}$$

$$\langle c_j c_{j'}^{\dagger}\rangle = \frac{1}{L}\sum_k \sin^2 \theta_k \cos[k(j - j')], \quad \text{(E21)}$$

$$\langle c_j^{\dagger}c_{j'}^{\dagger}\rangle = \frac{1}{L}\sum_k \sin \theta_k \cos \theta_k \sin[k(j' - j)], \quad \text{(E22)}$$

$$\langle c_j c_{j'}\rangle = \frac{1}{L}\sum_k \sin \theta_k \cos \theta_k \sin[k(j - j')]. \quad \text{(E23)}$$

If we write a generic projector as $P_j^{\uparrow/\downarrow} = a_{2j-1}a_{2j}$, where a is either c or $c^{\dagger}$, then

$$p_i = \mathrm{Pf}(\langle a_j a_{j'}\rangle)_{1 \leq i,j \leq 2L}. \quad \text{(E24)}$$

Notice that it is also possible to compute p_i when L is odd. The only difference is that the fermion number operator satisfies

$$\exp(i\pi\mathcal{N}) = -\mathcal{P}. \quad \text{(E25)}$$

Therefore, one has to take periodic boundary conditions $c_L^{\dagger} = c_0^{\dagger}$ and only keep configurations with an odd number of fermions. The wave vectors are now in the set $\{2l\pi/L\,|\,-L/2 \leq l \leq L/2 - 1\}$. Since the dispersion relation $\varepsilon(k)$ is minimum for $k = -\pi$, the ground-state wave function is

$$|\widetilde{0}\rangle = b_{-\pi}^{\dagger}|0\rangle, \quad \text{(E26)}$$

and the probabilities

$$p_i = \langle \widetilde{0}|P_1^{\uparrow/\downarrow}P_2^{\uparrow/\downarrow}\dots P_L^{\uparrow/\downarrow}|\widetilde{0}\rangle \quad \text{(E27)}$$

will also be given by Pfaffians.

3. Configuration with highest probability

We study the case where L is even. The configuration with highest probability is attained by the ferromagnetic configuration

$$|i_0\rangle = |\uparrow\uparrow\uparrow\dots\rangle_z. \quad \text{(E28)}$$

Defining

$$P = \prod_{j=0}^{L-1} c_j^{\dagger}c_j, \quad \text{(E29)}$$

p_0 is expressed as

$$p_0 = \langle 0|P|0\rangle. \quad \text{(E30)}$$

P is a projector onto a state with L fermions.

$$Q = \prod_k c_k^{\dagger}c_k \quad \text{(E31)}$$

is also a projector onto a state with L fermions. Since there is only *one* state of the Hilbert space with L fermions, P and Q are in fact identical. Using Eq. (E8), we therefore get

$$p_0 = \prod_k \cos \theta_k, \quad \text{(E32)}$$

where θ_k is given by Eq. (E13) or (E15). At the critical point $(\mu = 1)$, $\theta_k = k/4$.

[1] L. Amico, R. Fazio, A. Osterloh, and V. Vedral, Rev. Mod. Phys. **80**, 517 (2008).

[2] C. Holzhey, F. Larsen, and F. Wilczek, Nucl. Phys. B **424**, 443 (1994).

[3] G. Vidal, J. I. Latorre, E. Rico, and A. Kitaev, Phys. Rev. Lett. **90**, 227902 (2003).

[4] V. E. Korepin, Phys. Rev. Lett. **92**, 096402 (2004).

[5] P. Calabrese and J. Cardy, J. Stat. Mech.: Theory Exp. (2004), 06002.

[6] H. Casini and M. Huerta, Phys. Lett. B **600**, 142 (2004).

[7] S. Furukawa, V. Pasquier, and J. Shiraishi, Phys. Rev. Lett. **102**, 170602 (2009).

[8] P. Calabrese, J. Cardy, and E. Tonni, arXiv:0905.2069 (unpublished).

[9] A. Kitaev and J. Preskill, Phys. Rev. Lett. **96**, 110404 (2006).

[10] M. Levin and X.-G. Wen, Phys. Rev. Lett. **96**, 110405 (2006).

[11] M. Haque, O. Zozulya, and K. Schoutens, Phys. Rev. Lett. **98**, 060401 (2007); O. S. Zozulya, M. Haque, K. Schoutens, and E. H. Rezayi, Phys. Rev. B **76**, 125310 (2007).

[12] B. A. Friedman and G. C. Levine, Phys. Rev. B **78**, 035320 (2008).

[13] A. Hamma, R. Ionicioiu, and P. Zanardi, Phys. Lett. A **337**, 22 (2005); Phys. Rev. A **71**, 022315 (2005).

[14] S. Furukawa and G. Misguich, Phys. Rev. B **75**, 214407 (2007).

[15] C. Castelnovo and C. Chamon, Phys. Rev. B **76**, 174416 (2007).

[16] S. Papanikolaou, K. S. Raman, and E. Fradkin, Phys. Rev. B **76**, 224421 (2007).

[17] A. Hamma, W. Zhang, S. Haas, and D. A. Lidar, Phys. Rev. B **77**, 155111 (2008).

[18] N. Anantharaman and S. Nonnenmacher, Ann. Henri Poincare **8**, 37 (2007).

[19] Y. G. Sinai, Funct. Anal. Appl. **2**, 61 (1968).

[20] A measure of phase space which is invariant under a chaotic transformation can sometimes be represented by a probability distribution on the configurations of a spin chain.

[21] D. S. Rokhsar and S. A. Kivelson, Phys. Rev. Lett. **61**, 2376 (1988).

[22] C. L. Henley, J. Phys.: Condens. Matter **16**, S891 (2004).

[23] E. Fradkin and J. E. Moore, Phys. Rev. Lett. **97**, 050404 (2006).

[24] B. Hsu, M. Mulligan, E. Fradkin, and Eun-Ah Kim, Phys. Rev. B **79**, 115421 (2009).

[25] M. A. Metlitski, C. A. Fuertes, and S. Sachdev, arXiv:0904.4477 (unpublished).

[26] Here we take a standard notation used in statistical mechanics and field theory, where $R=1$ for a free fermion and $R=\sqrt{2}$ for a SU(2)-symmetric case. In condensed matter physics, a common notation is $R^{\mathrm{cm}}=R/\sqrt{4\pi}$, and the coupling constant $K=1/R^2$ known as TLL parameter is also widely used.

[27] F. J. Dyson, J. Math. Phys. **3**, 140 (1962); **3**, 157 (1962); **3**, 166 (1962).

[28] M. Gaudin, J. Phys. (France) **34**, 511 (1973).

[29] F. Calogero, J. Math. Phys. **10**, 2191 (1969).

[30] B. Sutherland, J. Math. Phys. **12**, 246 (1971).

[31] L. Campos Venuti, H. Saleur, and P. Zanardi, Phys. Rev. B **79**, 092405 (2009).

[32] R. Moessner, S. Sondhi, and P. Chandra, Phys. Rev. B **64**, 144416 (2001).

[33] R. Moessner and S. Sondhi, Phys. Rev. Lett. **86**, 1881 (2001).

[34] G. Misguich, D. Serban, and V. Pasquier, Phys. Rev. Lett. **89**, 137202 (2002).

[35] C. Castelnovo, C. Chamon, C. Mudry, and P. Pujol, Ann. Phys. (N.Y.) **322**, 903 (2007).

[36] E. Ardonne, P. Fendley, and E. Fradkin, Ann. Phys. (N.Y.) **310**, 493 (2004).

[37] It is interesting to notice that ρ_Ω ($\Omega=A,B$) is block diagonal in the spin basis, each block being labeled by a spin configuration i at the boundary. Block number i is a card $\mathcal{E}_i^\Omega \times$ card $\mathcal{E}_i^\Omega$ matrix and has only *one* nonzero eigenvalue p_i, the corresponding eigenvector being $|RK_i^\Omega\rangle$. In the special case where all the energies $E_\Omega(\omega,i)$ vanish, each state $|\mathrm{RK}_i^\Omega\rangle$ is an equal-amplitude superposition of spin configurations. Then, each block of ρ_Ω is particularly simple since all its matrix elements are *identical*. The block labeled by the boundary configuration i, of size card $\mathcal{E}_i^\Omega$ $\times$ card $\mathcal{E}_i^\Omega$, has all its entries equal to $p_i/$ card $\mathcal{E}_i^\Omega$ and a trace equal to p_i.

[38] Here the factor 2 is inserted because it will be convenient in Sec. III when identifying $E(i)$ as a Coulomb gas model. One may also think that the interactions occurring in A and B make a contribution $E(i)$ each and that the total contribution is twice of it.

[39] H. Li and F. D. M. Haldane, Phys. Rev. Lett. **101**, 010504 (2008).

[40] F. D. M. Haldane, Talk at KITP Conference, February 2009 (unpublished), http://online.kitp.ucsb.edu/online/lowdim_c09/haldane/

[41] The particle coordinates are restricted to be multiple of $2\pi/L$ ground-state wave function of the Calogero-Sutherland model.

[42] Y.-S. Wu and Y. Yu, Phys. Rev. Lett. **75**, 890 (1995).

[43] F. D. M. Haldane, Phys. Rev. Lett. **60**, 635 (1988).

[44] B. S. Shastry, Phys. Rev. Lett. **60**, 639 (1988).

[45] W. Nahm, Nucl. Phys. B **124**, 121 (1977).

[46] J. Polchinski, *String Theory* (Cambridge University Press, Cambridge, 1998).

[47] M. L. Mehta, *Random Matrices* (Academic Press, San Diego, 1991).

[48] A. Schmid, Phys. Rev. Lett. **51**, 1506 (1983).

[49] R. J. Baxter, *Exactly Solved Models in Statistical Mechanics* (Dover, Mineola, 1982).

[50] P. W. Kasteleyn, in *Fundamental Problems in Statistical Mechanics III*, edited by E. D. G. Cohen (North-Holland, Amsterdam, 1975), p. 103.

[51] T. Giamarchi, *Quantum Physics in One Dimension* (Oxford University Press, New York, 2004).

[52] D. C. Cabra, A. Honecker, and P. Pujol, Phys. Rev. B **58**, 6241 (1998).

[53] N. M. Bogoliubov, A. G. Izergin, and V. E. Korepin, Nucl. Phys. B **275**, 687 (1986).

[54] S. Qin, M. Fabrizio, L. Yu, M. Oshikawa, and I. Affleck, Phys. Rev. B **56**, 9766 (1997).

[55] N. Shannon, G. Misguich, and K. Penc, Phys. Rev. B **69**, 220403(R) (2004).

[56] F. Pollmann, J. J. Betouras, K. Shtengel, and P. Fulde, Phys. Rev. Lett. **97**, 170407 (2006).

[57] A. Y. Kitaev, Ann. Phys. (N.Y.) **303**, 2 (2003).

[58] H. A. Kramers and G. H. Wannier, Phys. Rev. **60**, 252 (1941).

[59] P. V. Buividovicha and M. I. Polikarpov, Phys. Lett. B **670**, 141 (2008).

[60] One can recall that at a certain value of R, the sine potential for ϕ becomes relevant and ϕ is locked at a constant value, leading to a crystallization. Conversely, a crystal state can be regarded as a ϕ-locked state.

[61] Note that for the dimer models on the square and hexagonal lattices, the radius of ϕ is given by $R=1$, not by $R=2$ used by Hsu *et al.* (Ref. 24).

[62] V. Petkova and J. Zuber, *Proceedings of "Nonperturbative Quantum Field Theoretic Methods and their Applications*," Budapest, Hungary, 14–21 August 2000, edited by Z. Horvath and L. Palla (World Scientific, Singapore, 2001), pp. 1–35.

[63] H. W. J. Blöte and H. J. Hilhorst, J. Phys. A **15**, L631 (1982); B. Nienhuis, H. J. Hilhorst, and H. W. J. Blöte, *ibid.* **17**, 3559 (1984).

[64] J. Kondev and C. L. Henley, Phys. Rev. B **52**, 6628 (1995); Nucl. Phys. B **464**, 540 (1996); C. Zeng and C. L. Henley, Phys. Rev. B **55**, 14935 (1997); R. Raghavan, C. L. Henley, and S. L. Arouh, J. Stat. Phys. **86**, 517 (1997).

[65] F. Alet, Y. Ikhlef, J. L. Jacobsen, G. Misguich, and V. Pasquier, Phys. Rev. E **74**, 041124 (2006).